

THE EFFECT OF OXYGEN ON THE MECHANICAL PROPERTIES
OF A B.C.C. TITANIUM ALLOY

by
WILLIAM DAVID ROSENBERG

B.Met.E. Rensselaer Polytechnic Institute 1963
M.S. Syracuse University 1966

Submitted in Partial Fulfillment
of the Requirement for the
Degree of
DOCTOR OF SCIENCE
at the
MASSACHUSETTS INSTITUTE OF TECHNOLOGY
1972

Signature of Author _____
Department of Metallurgy and Materials
Science, May 5, 1972

Certified by _____
Thesis Supervisor

Accepted by _____
Chairman, Departmental Committee on
Graduate Students

Archives



THE EFFECT OF OXYGEN ON THE MECHANICAL PROPERTIES
OF A B.C.C. TITANIUM ALLOY

by

WILLIAM DAVID ROSENBERG

Submitted to the Department of Metallurgy and Materials
Science on May 5, 1972 in partial fulfillment of the
requirements for the degree of Doctor of Science

.....

ABSTRACT

The influence of oxygen on the mechanical properties of a body-centered-cubic titanium-30 weight percent (17.7 atom percent) molybdenum-oxygen alloy has been investigated. Three levels of oxygen equivalents, 0.16, 0.81 and 2.07 atom percent, were considered in this study. The lattice constant was shown to increase by 0.0063 Å per atom percent oxygen. The role of oxygen in strengthening these alloys was shown to be athermal in nature over a temperature range of 77° to 538°K. Mechanical tests, augmented by transmission electron microscopy, were employed to study the dependence of strength upon grain size. Negligible grain boundary strengthening was found for the two alloys having the lowest oxygen content. Further, the dislocation density, at a given level of strain, was also found to be insensitive to grain size in the forenamed alloys. On the other hand, the highest oxygen content alloy exhibited significant grain boundary strengthening. The Hall-Petch slope, k , for yielding and flow stresses up to 10 percent strain were finite and nearly equal in this alloy. Further, the dislocation density was a function of grain size for this alloy. As predicted by a work hardening model for grain boundary strengthening, the strength and dislocation density should exhibit parallel dependences on grain size. The dislocation substructure developed in all alloys was identical in nature and consisted of screw dislocations arranged in slip bands. The slip plane and Burgers vector were shown in all alloys studied to be (211), and $1/2$ a $\langle 111 \rangle$, respectively. The absence of significant grain boundary strengthening in the two lower oxygen content alloys is rationalized in terms of the relative strength of the interaction between interstitial solutes with dislocations and the applied stress. The

interstitial solute-dislocation interaction forms a barrier which reduces the average slip distance, $\bar{\lambda}$, of a dislocation. The mechanical properties are controlled by interaction with this barrier and grain boundaries have minimal influence. The dislocation-interstitial interaction is surmounted at higher stress levels, as in the highest oxygen content alloy, and the slip distance is then controlled not by the solute separation but by the grain diameter. Mechanical behavior is then controlled by the grain boundary with a resulting dependence of both strength and dislocation density on grain size.

Thesis Supervisor: John F. Breedis

Title: Associate Professor of Metallurgy

TABLE OF CONTENTS

<u>Chapter Number</u>		<u>Page Number</u>
	ABSTRACT	2
	LIST OF FIGURES	6
	LIST OF TABLES	8
	ACKNOWLEDGEMENTS	9
1	INTRODUCTION	10
2	LITERATURE REVIEW	13
	A. Mechanical Properties of Titanium- Molybdenum	13
	B. Deformation of B.C.C. Metals	15
	C. Interstitial Strengthening of B.C.C. Metals	17
	D. Grain Boundary Strengthening	21
3	EXPERIMENTAL PROCEDURE	29
	A. Material Preparation	29
	B. Lattice Constant Determination	30
	C. Mechanical Test Specimen Preparation ..	32
	D. Mechanical Tests	33
	E. Electron Microscopy	34
4	RESULTS	38
	A. Lattice Constant Determination	38
	B. Comparison of Tension and Compression Tests	38
	C. Yield Strength Versus Temperature	40
	D. Compression Strength Versus Grain Size	43
	E. Electron Microscopy	52
5	DISCUSSION	61
	A. Lattice Constant Determination	61
	B. Comparison of Tension and Compression Tests	61
	C. Yield Strength Versus Temperature	62
	D. Grain Size Effects	67

<u>Chapter Number</u>		<u>Page Number</u>
6	CONCLUSIONS	79
7	SUGGESTIONS FOR FURTHER WORK	80
	REFERENCES	81
	BIOGRAPHICAL NOTE	85

LIST OF FIGURES

<u>Figure Number</u>		<u>Page Number</u>
1	The effect of oxygen on a portion of the percent molybdenum phase diagram	12
2	The effect of oxygen on the titanium-30 weight percent molybdenum lattice constant ..	39
3	The effect of temperature on the yield strength on alloys A, B and C	41
4	Typical true stress-true strain curves for alloys A, B and C	42
5	A plot of the yield strength of the alloys A, B and C, at various temperature versus the oxygen equivalent	44
6	A plot of the yield strength of alloys A, B and C at various temperatures versus the square root of the oxygen equivalent	45
7	Typical microstructures of titanium-30 weight percent molybdenum depicting the range of grain sizes studied. Magnification, 300X ...	46
8	The yield and flow stress dependence on grain size for alloy A	47
9	The yield and flow stress dependence on grain size for alloy B	48
10	The yield and flow stress dependence on grain size for alloy C	49
11	Typical dislocation structures observed in alloy A at 0.5 strain	53
12	Typical dislocation structures observed in alloy B at 2.0 strain	54
13	Typical dislocation structures observed in alloy C at 4.0 strain	55
14	The effect of strain on the dislocation density for alloys A and B	56
15	The effect of strain on the dislocation density for alloy C	57

<u>Figure Number</u>		<u>Page Number</u>
16	Flow stress versus the square of dislocation density for alloy C	59
17	Schematic diagram of the effect of an internal barrier on the grain size versus stress results	77

LIST OF TABLES

<u>Table Number</u>		<u>Page Number</u>
1	Values of the Strengthening Effect of Interstitials $\Delta\sigma/\Delta c$, Expressed in Terms of the Metals Shear Modulus, G	20
2	Values of σ_0 , the Function Stress and k_y , the Hall-Petch Slope for Yielding, for Some B.C.C. Metals	28
3	Interstitial Content of the Three Titanium-30 Weight Percent Molybdenum Alloys	30
4	Comparison of Tensile and Compressive Yield Strengths	40
5	Values of k, the Hall-Petch Slope, for Alloys A, B and C at Various Strains. Recrystallization Temperature Was 1100°C ...	50
6	Values of k, the Hall-Petch Slope, for Alloy A at Various Strains. Recrystallization Temperature Was 900°C	51
7	Dislocation Densities of Alloys A, B and C at Various Strains	58
8	Strengthening, Expressed as $\Delta\sigma/\Delta c$, and the Lattice Constant for Several B.C.C. Metals	65

ACKNOWLEDGEMENTS

The author is most grateful to Professor John F. Breedis for his patient guidance throughout this the completion of this work. He also wishes to thank Professor John Vander Sande and Robin Stevenson for helpful discussions concerning this work.

In addition, thanks are given to Miss Miriam Yoffa for the several tasks she performed including optical and electron microscopy sample preparation, printing the many micrographs necessary for the dislocation density measurements and the printing and mounting of the photomicrographs included in this work.

Finally, special thanks are in order for the author's wife, Rachel, who was willing to endure the life of a graduate student to make this work possible.

This work was sponsored by Air Force Contract AF-33/615/-3866. The author gratefully acknowledges this financial support throughout this work.

I. INTRODUCTION

Titanium and its alloys have been utilized in high performance applications where a high strength-to-weight ratio and excellent corrosion resistance are important. Much work has been devoted in the past to studying the effects of alloying additions to further improve strength. One of the most successful means of strengthening titanium has been through alloying to suppress the beta-to-alpha (body-centered cubic to hexagonal-close-packed) transformation. The b.c.c. phase in pure titanium is less dense than the h.c.p., but the amount of alloying element needed to suppress the beta-to-alpha transformation usually raises the density of the b.c.c. phase above the h.c.p. phase. As a result, the strengthening, when measured in terms of the strength-to-weight ratio, is not as great as when measured in terms of the yield strengths. For example, for a beta-phase alloy, titanium-3 weight percent aluminum-13 weight percent vanadium-11 weight percent chromium is 30 percent stronger than commercially pure alpha-phase titanium when measured in terms of yield strengths but only 24 percent stronger when measured in terms of strength-to-weight ratios.

Molybdenum was the beta stabilizing alloying element chosen in this work because of its potency in solid solution strengthening. The alloy used in this investigation contained 30 weight percent (17.7 atomic percent) molybdenum.

Another method of solid solution strengthening is by addition of an interstitial solute. The effect of interstitial atoms on body-centered-cubic metals can be particularly marked. Substantial increases in strength, the development of a yield point and a reduction in ductility are commonly observed as interstitial solutes are added. In titanium containing greater than 20 weight percent molybdenum, it is possible to dissolve one weight percent (3.4 atomic percent) oxygen at 1100°C (1). Figure 1 shows the effect of oxygen on titanium-30 molybdenum(1). Oxygen is an alpha stabilizer but the beta-phase can be retained by quenching even with one weight percent oxygen. This is due to the sluggish rate of transformation from beta to alpha. The relatively large solubility of oxygen led to its selection as the interstitial strengthener in this work.

The intent of this research is to investigate the effect of oxygen on the mechanical properties of a beta-titanium alloy. The effect of oxygen on several parameters were investigated, including the variation of the lattice constant with composition, the yield strength as a function of temperature, and the yield and flow strength as a function of grain size.

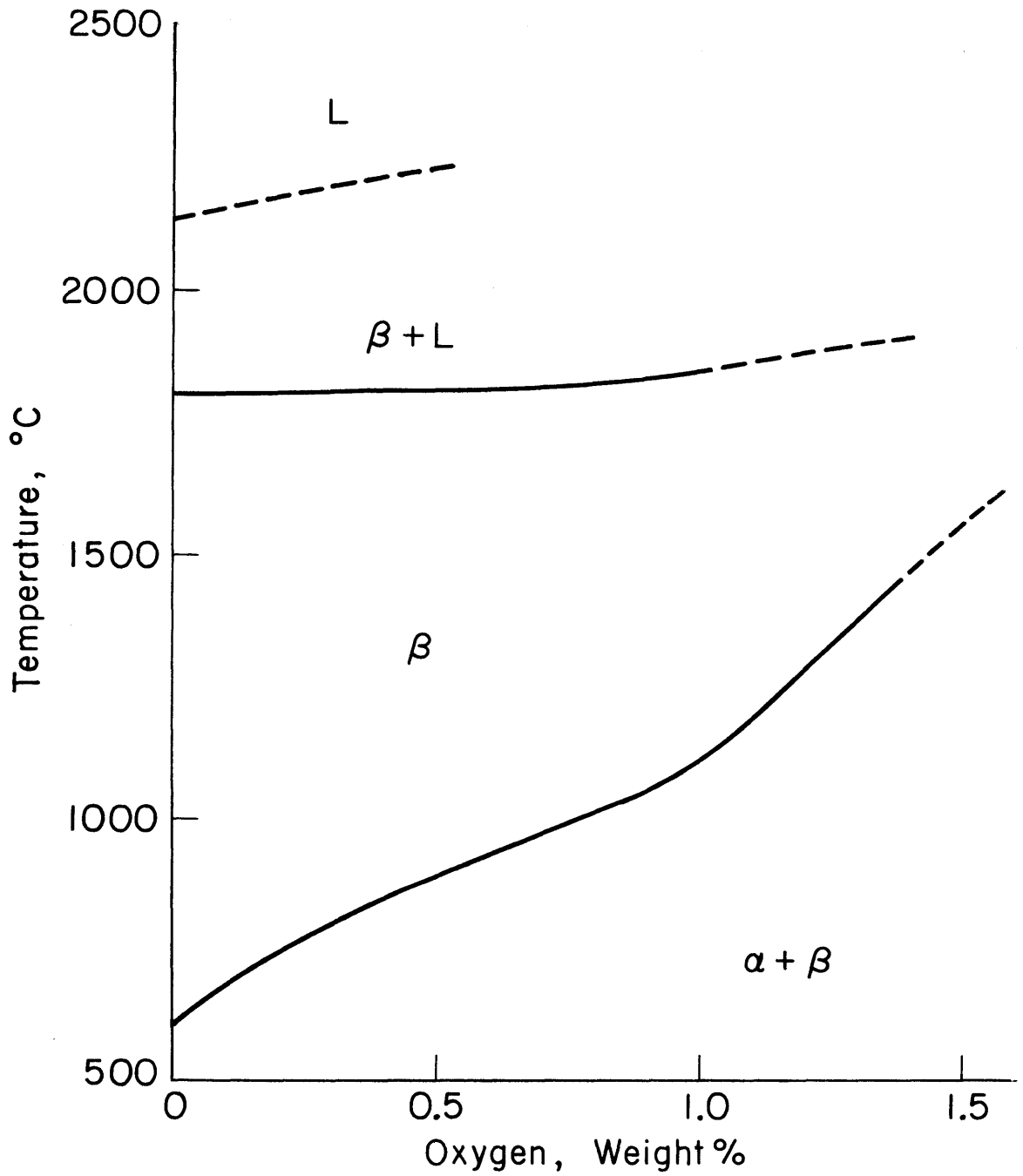


Figure 1: The effect of oxygen on a portion of the titanium-30 weight percent molybdenum phase diagram.

II. LITERATURE REVIEW

A. Mechanical Properties of Titanium-Molybdenum

Holden et al.(2) investigated titanium-molybdenum alloys over a range of composition from pure titanium to 24.5 weight percent molybdenum. They found that the yield strength in tension increased in other than a monotonic fashion over this range from 23 Kg/mm² to 70 Kg/mm². The yield strength increased over the range 0 to 5 weight percent molybdenum to 63 Kg/mm², then dropped to 32 Kg/mm² at 8 weight percent, and subsequently rose to its final value of 70 Kg/mm² at 24.5 weight percent molybdenum. The low yield strength in the 8-16 weight percent molybdenum region resulted from the low shear stresses required to initiate the transformation to martensite. As the molybdenum content increases, the stress required for this transformation increases to a point where it is greater than the critical shear stress for slip.

Stress-strain curves from the work of Holden et al show no yield drop for the b.c.c. alloys and the 24.5 weight percent molybdenum alloy exhibited linear work hardening up to fracture which occurred at 10 percent true strain.

Recently, Zeyfang and Conrad(3) investigated a titanium-26.4 weight percent molybdenum alloy with 0.5 atomic percent oxygen equivalent. Oxygen equivalents were calculated by taking nitrogen equals 2 oxygen and carbon equals 3/4 oxygen based on Conrad's earlier work(4).

Adding the nitrogen and carbon equivalents to the oxygen content then yielded an oxygen equivalent. They examined the effects of temperature and strain-rate on the flow behavior. The mechanical behavior of the alloy was generally similar to other interstitially strengthened b.c.c. metals except for the lack of an initial yield point. The strong effect of temperature on the yield stress at low temperatures was noted. Stress-strain curves similar to Holden's were also observed. The strain-rate sensitivity of the material was very low, and at 673⁰K, serrated yielding was noted.

Using thermal activation analysis, Zeyfang and Conrad concluded that the rate controlling process was one of mobile dislocations overcoming interstitials. The dislocation-interstitial interaction was described as consisting of two parts: (1) a chemical type of breaking titanium-interstitial bonds and (2) an elastic part describing overcoming the interstitial's elastic stress field. Tyson(5,6) first proposed this chemical contribution after calculating the interaction energy using the method of Cochardt et al.(7) and found the results insufficient to explain the observed interaction energy. Tyson's conclusion was that the breaking of chemical bonds in the dislocation core may be a significant source of strengthening in interstitial titanium-oxygen alloys.

B. Deformation of B.C.C. Metals

The deformation of b.c.c. metals has been a much-studied phenomenon. A recent extensive review by Christian(8) covers the scope of this area. The object here will be to review those areas which are pertinent to this work rather than review the entire field.

One area of great interest in b.c.c. metals is the dependence of the flow stress on temperature in the low temperature region. The controversy over whether the low temperature strength is due to an intrinsic lattice resistance, the Peierls-Nabarro force, or to dispersed interstitial solutes is still not fully resolved. Ravi and Gibala(9) have concluded from their results on niobium-oxygen alloys that all of the low temperature strength is due to interstitial hardening. They obtained a value for the yield stress at zero oxygen content through extrapolation of their curve for stress versus concentration. This method has been criticized by Christian(8). Christian points out that the stress obtained by Ravi and Gibala at 77⁰K with their technique is about one-half that obtained by two other independent measurements on presumably interstitial-free crystals. In order to resolve the question of inherent lattice hardening or interstitial strengthening, purer metals and alloys are needed.

B.C.C. metals can slip on several systems. The Burgers vector most often observed is $1/2 a \langle 111 \rangle$. However, evidence for some slip on a $\langle 110 \rangle$ and $\langle 100 \rangle$ has been reported(10,11). The densities of the two latter types of dislocations are usually very low and thought to result from $1/2 a \langle 111 \rangle$ reactions. The planes observed have included $\{110\}$, $\{112\}$, $\{123\}$, as well as irrational planes. The two planes most often observed are the $\{110\}$ and $\{112\}$. For titanium-vanadium alloys containing between 20 and 50 atom percent vanadium, Paton and Williams(12) noted a slip plane between $(\bar{3}12)$ and $(\bar{2}11)$ poles. Koul(13) noted slip in titanium-26 weight percent molybdenum on what appeared to be $\{112\}$ planes.

Like the yield stress, the dislocation structure of b.c.c. metals is dependent on temperature and alloy content. Foxall and Statham(14) made a detailed study of the effect of temperature and molybdenum content on the dislocation structure in niobium single crystals. They found that increasing the yield stress by lowering the temperature or increasing the molybdenum content (up to 16 atom percent molybdenum) increased the proportion of observed screw dislocations. The screw dislocations at high yield stresses were straight and very long. As the stress was lowered, the screw dislocations became wavy with more "debris". Edge dipoles formed at even lower stresses. Paton and Williams(12) and Gelles(15) studied polycrystalline

titanium-vanadium dislocation structures. At low temperatures, between 77⁰K and room temperature, both observed screw dislocations in bands. As the temperature was raised up to 440⁰K, the screw dislocations became wavy in appearance and the dislocation density decreased for the same level of strain. Koul(13) also observed bands of straight screw dislocations in titanium-26 weight percent molybdenum strained at room temperature.

C. Interstitial Strengthening of B.C.C. Metals

One of the most important characteristics of b.c.c. metals is their ability to be substantially strengthened by interstitial solutes. Two types of models have been proposed to explain such strengthening. One type involves a Cottrell interaction between a dislocation and an interstitial atom (such as the theories of Petch(16,17), Friedel(18,19) and Fleischer(20)) while the other type involves the concept of Snoek ordering(21) (such as the theory of Schoek and Seeger(22)).

The Petch model predicts a linear relationship between yield stress and interstitial concentration. The linear relationship is, however, only valid for very low concentrations (0.005 - 0.025 weight percent).

The Friedel theory predicts a $C^{1/3}$ relationship with yield stress. This model assumes an elastic interaction even at small separations between interstitial and dislocation, and assumes isotropic elasticity. The stress calculated is assumed to be that necessary to unpin a

dislocation from the interstitial atoms.

Fleischer's model uses the interaction of interstitial and dislocation calculations proposed by Cochardt et al(7). This theory is based on short range interactions between dislocations and the tetragonal strain fields of interstitials. It predicts a temperature dependent strengthening that is proportional to $C^{1/2}$.

According to the Schoek and Seeger theory, large, elastic, long range interactions occur in b.c.c. crystals between dislocations and point defects. These defects characteristically possess asymmetrical strain fields in such metals. This interaction is the same as used by the Fleischer model above and is according to Cochardt et al. Due to these interactions, the interstitials, which are considered as elastic dipoles, become oriented in the energetically most favorable positions relative to the stress fields of the dislocations. These ordered atmospheres are referred to as Snoek atmospheres and are frozen-in at sufficiently low temperatures, such as room temperature. The stress necessary to drag the dislocations away from the atmosphere is linearly proportional to the concentration of interstitials and is independent of temperature with this approach.

The data in the literature has not resolved the issue of which theory is correct. Petch's model seems most invalid since in the low concentration regions it predicts a linear dependence whereas $C^{1/2}$ or $C^{1/3}$ dependences

are usually observed. The linear dependence between the solute concentration and yield stress is generally observed when a wide range of interstitial content (up to 1 atom percent) is investigated. Some systems exhibit different relationships between concentration and yield strength, dependent upon the concentration. The $C^{1/2}$ dependence is observed for low concentrations while a C dependence is observed for higher concentrations. The data for tantalum-nitrogen(23), tantalum-oxygen(24), niobium-oxygen(25,26) and niobium-nitrogen(25) all exhibit this dual dependence. Werts(27) data for carbon in iron shows a $C^{1/2}$ dependence but here the range of carbon concentration is only up to 0.0002 atom fraction. One notable instance of data showing a $C^{1/2}$ dependence is that of Owen and Roberts(28) where the range of dissolved carbon in martensitic iron-21 percent nickel is up to 0.08 atom fraction. In addition to the tantalum and niobium data mentioned above, the data for carbon and nitrogen combined in iron(30) and oxygen or nitrogen in vanadium(31) exhibit a linear dependence between strength and interstitial concentration.

Another important point to note is that even though the Cottrell interaction theories are short range in nature and, therefore, subject to thermal activation, a temperature dependent interaction has not been observed in any of the alloys mentioned above. The Schoek and Seeger theory, however, correctly predicts that the interstitial-dislocation interaction is unaffected by temperature.

The amount of strengthening, measured in terms of the shear modulus, G , appears to be related to whether C or $C^{1/2}$ dependence is observed. Values for the strengthening when C and $C^{1/2}$ dependences are observed, are shown below. There is an obvious difference then between the two dependences.

Table I

Values of the Strengthening Affect of Interstitials, $\Delta\sigma/\Delta C$, Expressed in Terms of the Metals Shear Modulus, G .

<u>concentration dependence</u>	<u>alloy system</u>	<u>strengthening in terms of the metal's shear modulus</u>
$C^{1/2}$	Fe-C	5 G
	Nb-N	2 G
C	Nb-N	0.5 G
	Nb-O	0.3 G
	Ta-N	0.3 G
	Ta-O	0.2 G

The question of the site in which the interstitial solute atom resides has not been discussed extensively in the literature. The interstitial solute is usually assumed to be in the octahedral site. The other site available is the tetrahedral position. In b.c.c. metals interstitial solutes in either site develop an asymmetrical lattice distortion. The tetrahedral site is, however, twice as large as the octahedral site. Expressed in terms of the

lattice constant, a spherical atom whose radius $0.126a$ can just be accommodated in the tetrahedral site while a smaller radius of $0.067a$ will just fit in the octahedral site. Beshers(29) has questioned the validity of the assumption that the octahedral site is the main occupation site for interstitials in some b.c.c. metals. Based on his calculations, Beshers has concluded that while carbon should occupy the octahedral site in iron, oxygen occupies the tetrahedral position in tantalum and niobium. Tetrahedral site occupation would produce less lattice distortion and would account for the lower values of strengthening observed in tantalum and niobium strengthened with oxygen versus carbon in iron. It must also be remembered however, that the lattice constants for niobium and tantalum are larger in comparison with that of iron and that this fact alone could account for the observed difference in strengthening.

D. Grain-Boundary Strengthening

Since the work of Hall(30) and Petch(31), much work has been undertaken to understand the linear relationship between the stress and the reciprocal square root of the grain size. The form of the equation is:

$$\sigma = \sigma_0 + kd^{-1/2} \quad (1)$$

with σ the yield, flow or fracture stress; σ_0 , a form of friction stress; k , the Hall-Petch slope designated k_y , for

yield, k_f for flow or fracture stress and; d , the grain size. This area of research has been reviewed in a series of papers(32). Much of this review is based on one of those papers(33).

The theories explaining the strengthening effect of grain boundaries fall into two categories: (1) pile-up theories, (2) non-pile-up theories. The pile-up theories were proposed to account for the grain size dependence of the lower yield stress in ferrite(32,33). A k_y value is then calculated using these theories. For the non-pile-up theories, it is the flow stress that is related to the grain size. The Hall-Petch slope for non-pile-up theories is k_f . One distinction between the two types of theories is that one predicts a k value for yielding while the other predicts a k value for the flow stress, i.e., a k_y and k_f value, respectively. The original pile-up theory of Petch(31) evolved from the work by Eshelby, Frank and Nabarro(34). They gave exact solutions for the stress ahead of a single layer, single ended pile-up of dislocations. The stress at the tip of the pile-up on one side of a grain boundary was thought to nucleate slip in the adjacent grain at some critical stress, σ_c . Eshelby et al. showed that the force, σ , on a dislocation due to a pile-up is given by:

$$\sigma = \frac{2nA}{\ell} \quad (2)$$

where n is the number of dislocations in the pile-up, A is a numerical constant which for screw dislocations = $\frac{Gb}{2\pi}$

(G is the shear modulus and b is the Burgers vector), ℓ is the length of the pile-up. At equilibrium;

$$(\sigma_{\text{tip}} - \sigma)b = (n - 1)\sigma b \quad (3)$$

and, therefore,

$$\sigma_{\text{tip}} = n\sigma \quad (4)$$

Petch used these results and equated σ_{tip} to σ_c and assumed that the length of the pile-up was equivalent to the grain diameter. Using the fact that $n = \sigma_c/\sigma$ and solving for σ with a friction stress, σ_0 , included to account for a resistance to dislocation motion within the grain, results in the Hall-Petch relationship;

$$\sigma = \sigma_0 + \sqrt{2A\sigma_c} d^{-1/2} \quad (5)$$

Later modifications have been made to include the fact that the pinned dislocation might have a different Burgers vector(35). Another approach has been to consider the pile-up as a continuous distribution of dislocations(36,37). Other types of pile-ups have also been considered. The main result has been, however, an equation of the form of the Hall-Petch equation with different numerical parameters included in the calculation of k , the Hall-Petch slope.

One type of non-pile-up theory proposed is based upon a work hardening model(38,39). The hardening introduced by grain boundaries is thought to be indirect.

The strength is related to the square root of the dislocation density through the equation;

$$\sigma = \sigma_0 + \alpha G b \rho^{1/2}, \quad (6)$$

where α is a numerical constant and ρ is the average dislocation density. This approach predicts that at a constant stress, all grain sizes will have the same dislocation density. This implies that the role of grain boundaries is to change the dislocation density. The dislocation density is then the controlling factor over the stress level. This argument is developed as follows: The average slip distance a dislocation moves, $\tilde{\lambda}$, is proportional to the grain size,

$$\tilde{\lambda} = \beta d \quad (7)$$

and the plastic strain is given by,

$$\epsilon = \rho b \tilde{\lambda} \quad (8)$$

combining equation (7) and (8) yields,

$$\rho = \rho_0 + \frac{\epsilon}{b \beta d} \quad (9)$$

where ρ_0 is the initial dislocation density. Substituting for ρ in equation (6) yields;

$$\sigma = \sigma_0 + \alpha G b \left(\rho_0 + \frac{\epsilon}{b \beta d} \right)^{1/2} \quad (10)$$

If the initial density, $\rho_0 \ll \epsilon b/\beta d$ then equation (10) reduces to:

$$\sigma = \sigma_0 + \alpha G \sqrt{\frac{b\epsilon}{\beta}} d^{-1/2} \quad (11)$$

which is equivalent to equation (1) with

$$k = \alpha G \left(\frac{b\epsilon}{\beta}\right)^{1/2} \quad (12)$$

Another non-pile-up theory was proposed by Li(40). In his approach, grain boundaries are assumed to act as sources of dislocations. The role of the grain boundary is important in this instance since with increasing grain boundary area, i.e. finer grain size, more dislocations will be emitted and hence the level of stress will be higher. Assuming m is the length of dislocation emitted per unit area of grain boundary, the density of dislocations is, for a spherical grain,

$$\rho = \frac{\frac{1}{2}(\pi d^2 m)}{\frac{1}{6} \pi d^3} = \frac{3m}{d} \quad (13)$$

where all terms have the aforementioned meaning and the factor of 1/2 arises due to the fact that the boundary is shared by two grains. Substituting equation (10) into equation (3) yields,

$$\sigma = \sigma_0 + \alpha G b (3m)^{1/2} d^{-1/2} \quad (14)$$

which is the same as the Hall-Petch relation with a slope,

$$k = \alpha G b (3m)^{1/2} \quad (15)$$

The pile-up model for explaining grain-boundary strengthening is now questioned as to its validity. For one thing, the lack of observation of pile-ups in pure metals whereas a Hall-Petch relation exists is a serious shortcoming. A second point is that in iron-3% silicon Worthington and Smith(41) found dislocations emitted from grain boundaries without the assistance of pile-ups. In addition, Worthington and Smith found that the stresses necessary to generate these dislocations were not a function of grain size. If dislocations can be generated without the aid of a pile-up and at stresses below the yield stress, the applicability of a model based on pile-ups generating dislocations which induce yielding is of questionable validity.

The work hardening theory has been criticized for its dependence on a material which shows parabolic hardening whereas not all materials possess this characteristic behavior. Another problem with this particular approach is that it predicts a strain independent friction stress, σ_0 , whereas this stress factor has been observed to increase in most metals investigated.

The main deterrent to acceptance of the Li theory has been the lack of abundant physical evidence to support it. Only a few instances of grain boundaries acting as sources of dislocations have been noted.

One important point with respect to this work is the fact that each theory includes in its development the average slip distance in some form. It is assumed that prior to, or at yielding, dislocations have moved from their source to grain boundaries. This is the basis for replacing the slip distance with some distance related to the grain diameter. This average slip distance is not a well defined quantity. Kocks(42) states that it is a quantity typically varying from 10 to 100 μ and is inversely proportional to stress. Measurements of this quantity in nickel(43) showed it to be as small as 6 μ at 30 Kg/mm². It is obvious then that replacement of the mean slip distance with the grain diameter is not valid for cases of higher yield strengths than 30 Kg/mm² and grain sizes greater than 6 μ .

The value of k , the Hall-Petch slope, would appear to be a constant in all the above theories for a given metal. This, however, is not the case for all metals. Typical values of k_y are listed below for some b.c.c. metals. As shown, the value for k_y generally varies from 0 to 3 Kg/mm^{3/2}. For f.c.c. and h.c.p., the values are from 0 to 1 and 0 to 1.5 Kg/mm^{3/2}, respectively. As shown, the value of k_y can change for one metal. The variation in the k_y value for niobium will be discussed later in the discussion. Tantalum-oxygen and iron-carbon alloys have a variable k_y which is dependent upon the heat treatment. Quenching samples from a region where the interstitial is in solution

Table II

Values of σ_0 , the Friction Stress, and k_y ,
the Hall-Petch Slope, for Yielding for Some B.C.C. Metals

<u>metal</u>	σ_0 <u>Kg/mm²</u>	k_y <u>Kg/mm^{3/2}</u>	<u>reference</u>
mild steel	7.2	2.39	44
Swedish iron	4.8	2.28	16
Swedish iron (no yield)	3.7	0.66	44
iron-carbon	5.4, 11.0	0.76, 2.9	52
chromium	18.2	2.90	45
tungsten	65.3	2.54	46
vanadium	32.5	0.98	47
niobium	7.0	~0 to 1.13	48, 49
tantalum-oxygen	19.0	~0 to 2.06	50, 51

results in a lower k_y compared with samples that have been quenched from lower temperatures or quenched and aged. Formby and Owen(51) rationalized this change as due to the formation of atmospheres around dislocations in the metal.

III. EXPERIMENTAL PROCEDURE

A. Material Preparation

Three alloys of titanium-30 wt. % molybdenum of differing oxygen content were prepared by the Battelle Memorial Institute. Electrolytic grades of titanium and a CMK-WB-2 grade of molybdenum were used in preparing the alloys. A master alloy was made first by a multiple arc-melting technique. The alloy was then homogenized and later diluted with oxygen and titanium to achieve the compositions desired.

The final ingot form was finger shaped having a length of 100 mm. and a diameter of roughly 20 mm. After grinding and/or machining, the alloys were rolled and hot swaged to reduce the diameter approximately 10 mm. The temperature for these operations was about 1000°C. The rods were subsequently machined to 6.3 mm. (0.25 in.) in diameter. Final preparation of the rod was carried out at M.I.T.

Examination of the alloys by optical microscopy revealed they were single phased with a grain size of 50 μ . Chemical analyses of the alloys studied is shown in Table III. The oxygen content was determined by neutron activation while the carbon content and nitrogen content were evaluated spectrographically. Oxygen equivalents were calculated by the method mentioned earlier using Conrad's(53)

values for the relative strengthening effect of carbon and nitrogen.

Table III
Interstitial Content of the Three
Titanium-30 Weight Percent Molybdenum Alloys

<u>alloy</u>	<u>oxygen (ppm)</u>	<u>nitrogen (ppm)</u>	<u>carbon (ppm)</u>	<u>oxygen equivalent atom fraction x 10⁻²</u>
A	344	37	92	0.16
B	1600	252	170	0.81
C	5000	347	170	2.07

B. Lattice Constant Determination

The change in lattice constant of the titanium-30 wt. % molybdenum alloy was measured as a function of oxygen content. The Debye-Scherrer technique was employed using both powder and solid specimens.

Initial measurements were made from powders. After filing, a magnet was used to separate the iron contamination introduced by the file from the alloy. After passing the filings through a 325 mesh screen, they were wrapped in titanium sheet several mils in thickness. The filings were annealed by encapsulating them in quartz which was evacuated to 3×10^{-5} torr and back filled with ultra-pure argon after purging three times. After the heat treatment of 30 minutes at 1100°C , the capsules were quenched in cold water. In addition to annealing, the high temperature

treatment served to insure that oxygen was completely in solution.

Solid specimens were used when it was found that oxygen was lost from powders during heat treatment. The solid specimens were prepared from heat treated 63 mm. rods which were then machined to 1 mm. in diameter, taking care to introduce as little strain as possible. These rods then were electropolished to 0.5 mm. in diameter or less.

Diffraction patterns were obtained using a 114.6 mm. in diameter camera. Both copper and cobalt radiation were employed in each exposure to increase the number of lines obtained. The double exposure introduced the problem of resolving the high angle lines from the background. The use of a copper filter for the copper radiation and a nickel filter for the cobalt radiation resulted in a significant reduction in background intensity while still retaining beta lines of both radiations. Using this technique with a powder or solid sample yielded as many as 26 lines of the possible 32 lines (including doublets).

The lattice constant for each specimen was determined through the use of a computer program(54). The program used a least-squares technique with correction terms included to compensate for: (1) film shrinkage, (2) specimen absorption, and (3) camera eccentricity. Reproducibility was demonstrated both by remeasuring the lines and by making several exposures.

C. Mechanical Test Specimen Preparation

Three series of mechanical tests were performed. The specimen for each was prepared in a slightly different manner. Tensile-type specimens were prepared for the tension versus compression tests while compression specimens were prepared for the tests at various temperatures and of various grain sizes.

The tensile-type specimens were 42 mm. long with a 3.5 mm. diameter. They were machined from the 6.3 mm. in diameter rods. Heat treatment was done for 30 minutes at 1100°C in a quartz capsule that had been evacuated to 3×10^{-4} torr and backfilled with ultra-pure argon at least three times. The gauge section of the tensile samples was then electropolished in a solution of 150 ml. methanol, 90 ml. n-butyl alcohol, and 15 ml. perchloric acid at less than -40°C .

Compression specimens for testing at various temperatures were 6.30 mm. in length and 3.15 mm. in diameter (height to diameter ratio = 2). The specimen ends were cut perpendicular to the compression axis through the use of a spark cutter. A right angle gauge showed that less than a degree error was possible when care was exercised. The heat treatment and encapsulation procedure were as described for the tensile specimens.

Samples of all three alloys were prepared with grain sizes of 5 to 100μ , measured using the linear intercept

method. For alloys A and B, the 6.3 mm. in diameter rod was cold swaged to 4.8 mm. in order to introduce cold work. Samples were recrystallized at 900 and 1100°C. Alloy C could not be cold worked satisfactorily; a reduction of less than 1 percent produced severe cracking. Cold work was introduced into this alloy by compressing 12.5 mm. long and 6.3 mm. in diameter samples to 2/3 of their original height. 950 and 1100°C were the recrystallization temperatures used for alloy C. The encapsulation procedure was identical to that described above. Subsequent to recrystallization, the samples were machined, electropolished and spark cut into samples. Alloys A and B had a height-to-diameter ratio of 2 (6.3 mm. long, 3.15 mm. in diameter) while alloy C had a height-to-diameter ratio of 1.5 (4.77 mm. long, 3.15 mm. in diameter).

Some samples of alloys A and C were aged after recrystallization. Instead of breaking the argon backfilled capsule in water after recrystallization as had been the procedure, the capsule was immersed in cold water until the sample had cooled to room temperature. The capsule was then aged for 30 minutes at 450°C. A quench produced by breaking the capsule under water followed the aging treatment.

D. Mechanical Tests

1. Tensile-Compression Test.

These tests were performed in an Instron machine using an apparatus designed to test the sample in tension

or compression. A ball and socket arrangement, designed by Stevenson(55), facilitated alignment so as to prevent buckling in compression. All tests were performed at a strain rate of $3 \times 10^{-4} \text{ sec}^{-1}$.

2. Compression Testing at Various Temperatures.

Compression tests were conducted in an Instron machine at various temperatures. The apparatus has been described previously by Gelles(15). The temperature range was 77°K to 538°K . The strain rate was $3 \times 10^{-4} \text{ sec}^{-1}$. The temperatures below 298°K were established by immersing the sample and testing rig in a suitable liquid bath; temperatures above room temperature were achieved through the use of a radiant heater in an enclosed environment.

3. Compression Testing of Various Grain Sizes.

A Tinius Olsen machine was used for compressing all the samples of alloys A, B and C recrystallized at 1100°C . An Instron machine was used for the alloys A and B which had been recrystallized at 900°C . The strain rate for all samples was $3 \times 10^{-4} \text{ sec}^{-1}$. Samples were strained various amounts up to 15 percent. Two layers of 0.025 mm. thick teflon were used for lubricating the ends of the specimen. The load was measured on the recorder in each of the machines.

E. Electron Microscopy

1. Preparation of Thin Foils.

Sections 0.2 mm. thick were cut from alloys A, B and

C that were tested as a function of grain size. The coarsest and finest grain size samples were used and strains of 0.5, 2.0, 4.0, 6.0 and 10.0 were investigated. The sections were cut perpendicular to the compression axis.

Thin foils were prepared from these blanks by means of electropolishing. The electrolyte used was that developed by Gelles(15) and is composed of 100 mil. lactic acid, 20 mil. hydrofluoric acid, and 10 mil. sulfuric acid. The solution was maintained at 20°C. The blanks were held in the solution by a pair of tweezers which gripped the sample at its edge. The edge of the foil blanks, as well as the tweezers, were masked with "Microstop" so as to expose only the center of the top and bottom of both faces to the solution. Polishing at 5 volts with rapid stirring close to these blanks was continued until perforation occurred. After perforation, the foil was washed in methanol. The lacquer was then stripped from the foil and repeated washings were done, first in methanol and distilled water and then in distilled water and "Crystal Kleen". The "Crystal Kleen" was washed from the foil with methanol and the foil was dried. Foils were stored under vacuum in a desiccator.

2. Dislocation Density Measurements.

Dislocation density measurements were made on alloys A, B and C recrystallized at 1100°C. Pictures were taken of dislocation structures using a (200) reflection. This reflection images all dislocations with $\frac{1}{2} a \langle 111 \rangle$ Burgers

vectors. For each measurement, pictures from at least two foils and from at least two grains in each foil were used. A total of ten pictures for each condition were measured. The technique used was that described by Steeds(56). Ten circles of equal radius were randomly placed on the pictures. Intersections with the circles were then counted. A total of 100 measurements per condition was recorded. The foil thickness could not be measured directly in this material, but was estimated from observed transmitted intensity. All micrographs were taken at approximately the same estimated foil thickness of 2000 Å. For the 0.5 percent strains, a magnification of 33,000X was employed while a magnification of 64,000X was used for larger strains.

From the pictures it was obvious that the distribution was non-random and, therefore, the dislocation density is given by

$$\rho = \frac{NM}{2tD} \text{ in cm/cm}^3 \quad (16)$$

where ρ is the dislocation density in centimeters per cubic centimeters, N is the number of intersections between dislocation and test line, M is the magnification, D is the diameter of the test circle and t is the assumed thickness of the foil.

3. Slip Plane Determination.

The slip plane was determined for both the A and C alloys at various strains. The technique involved finding a

major orientation when the foil had zero tilt. The assumption made then was that the foil area observed had its top and bottom surface perpendicular to the beam. Therefore, any intersection of the slip plane with the surface could be related to the orientation of the foil.

Pictures were taken of dislocations and of the corresponding diffraction patterns. Since the dislocations occurred in bands, a line drawn through their intersection with the surface defined a line in the slip plane. This line was projected onto the diffraction pattern after appropriate rotation to account for the difference in intermediate lens current. The angle between the trace of the slip plane and known planes was then measured from the plate. The slip plane was then determined with the aid of a stereographic projection.

4. Burgers Vector Determination.

The Burgers vector was determined using the no-contrast, $g \cdot b = 0$ criterion. This condition is valid generally only when working with screw dislocations since with edge dislocations residual contrast may be observed(57). Various reflections were used until a reflection did not image the dislocations. The diffraction patterns and bright field images were photographed and these were superimposed. The Burgers vector was then determined with respect to the dislocation image.

IV. RESULTS

A. Lattice Constant Determination

The results of the lattice constant determination are shown in Figure 2 where values of this constant are plotted versus the oxygen content, given in atomic percent. The lattice constant increase is linear with respect to oxygen concentration with a slope of 0.006 \AA per atomic percent oxygen. The lattice constants determined at 0.68 and 1.74 atomic percent oxygen are the result of measurements from solid specimens while the constant determined at near zero oxygen content was from a powder sample. As described earlier, powder samples were made from all three alloys. The lattice constant determined from the powders was approximately the same value as shown in the figure for zero oxygen content. Even sampling from the center of a large amount of powder (one gram) produced a lattice constant of similar magnitude to the other powder determinations. It was concluded that the titanium sheet encasing the powder was getting the oxygen from the sample.

B. Comparison of Tension and Compression Tests

The results of mechanical tests are shown below in Table IV. Normally, the yield strength in tension is the same as in compression. Within experimental error, the

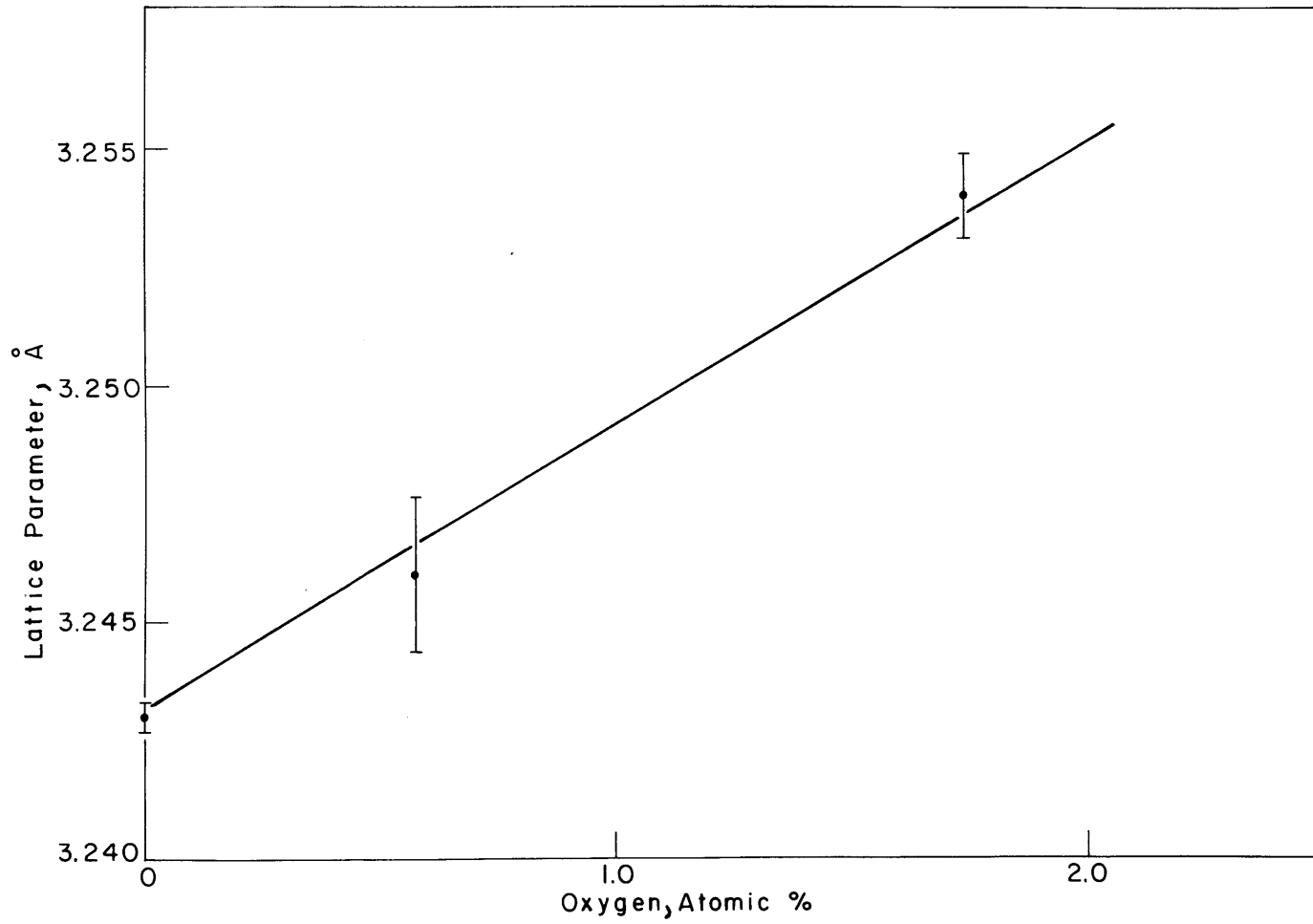


Figure 2: The effect of oxygen on the titanium-30 weight percent molybdenum lattice constant.

results here are the same also, except for alloy C, where brittle fracture occurred in tension. The limited tensile elongation in alloy C indicated further testing would necessarily be done in compression.

Table IV
Comparison of Tensile and Compression
Yield Strengths

<u>alloy</u>	<u>type of test</u>	<u>yield strength 0.2% offset Kg/mm²</u>
A	compression	63
	tensile	70
B	compression	88
	tensile	90
C	compression	114
	tensile	60 ^a

(a) brittle fracture

C. Yield Strength Versus Temperature

Figure 3 shows the yield strength of the three alloys plotted versus testing temperature. All three curves show the same dependence of yield strength on temperature. The three oxygen levels affect only the athermal behavior of alloy. The true stress-true strain curves typical of the three alloys are illustrated in Figure 4. These curves were drawn from the room temperature test results but represent the character of the curves obtained throughout the temperature range investigated. No

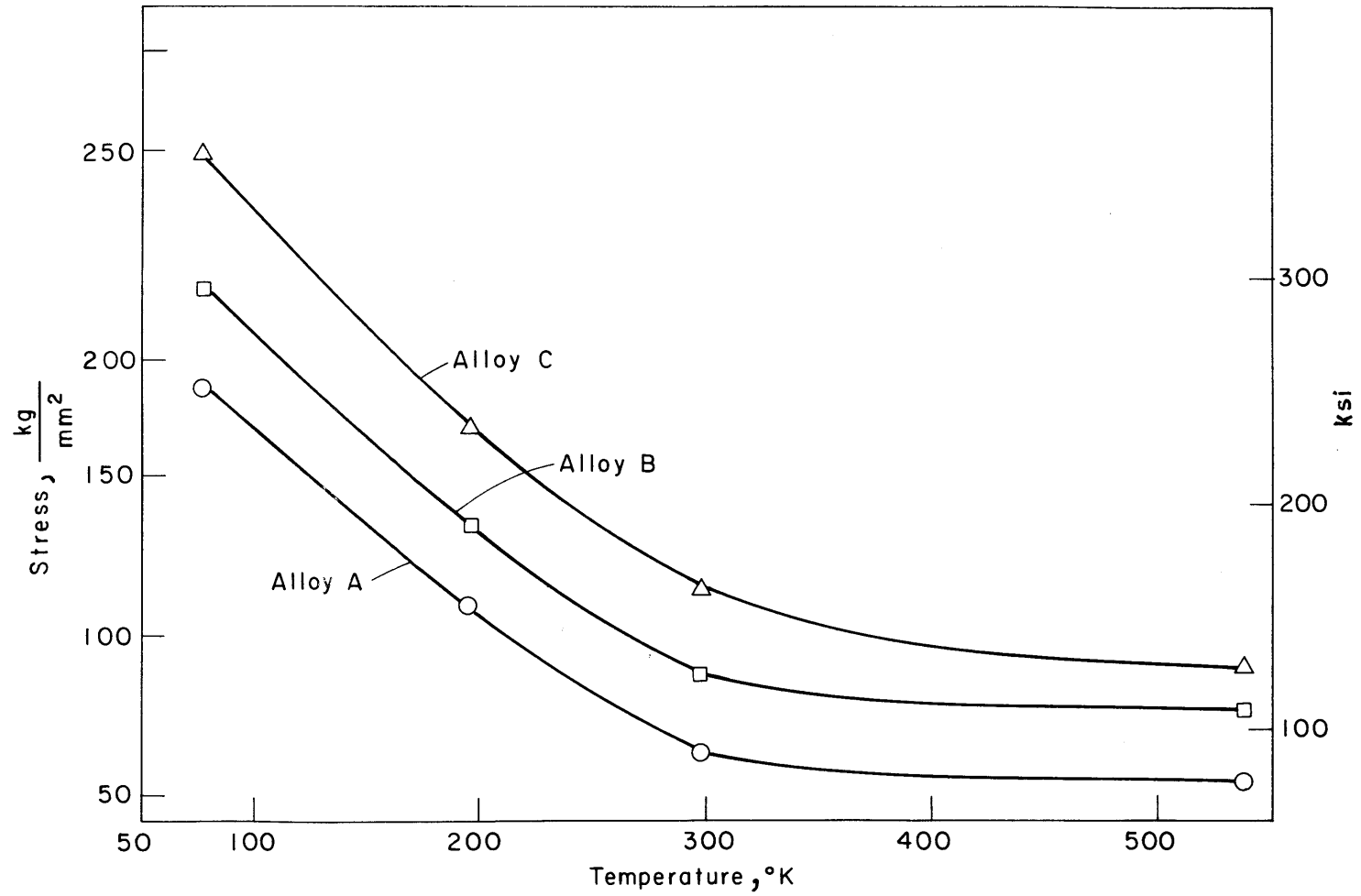


Figure 3: The effect of temperature on the yield strength on alloys A, B and C.

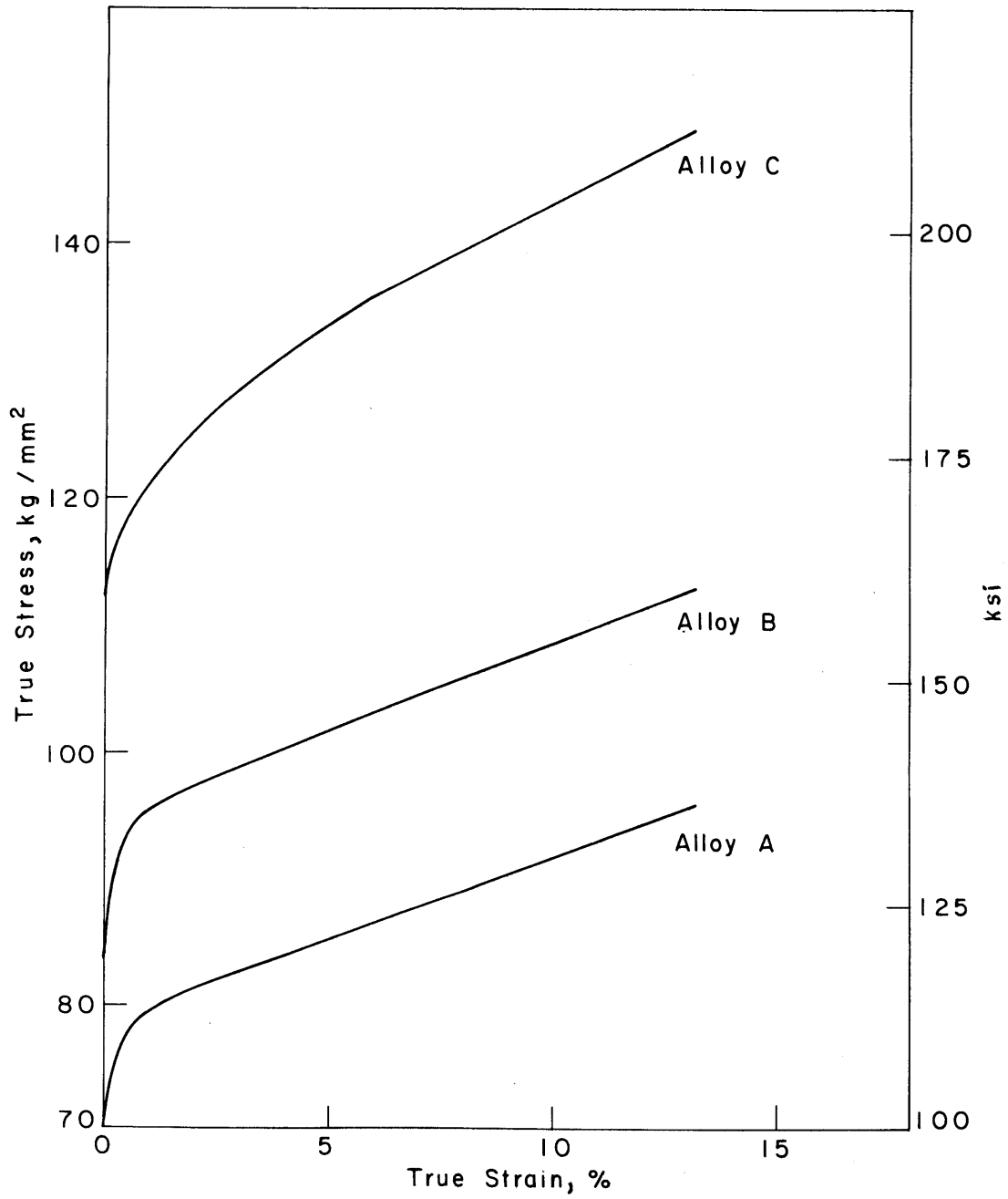


Figure 4: Typical true stress-true strain curves for alloys A, B and C.

yield drop was noted for any of the alloys at any temperature and the rate of linear work hardening was the same for all temperatures at 1.4×10^{-3} G (68 Kg/mm^2 or 9.7×10^4 Ksi).

Figures 5 and 6 show the yield strength plotted as functions of oxygen equivalent to the first and one-half power, respectively. It is obvious one could claim a fit to either composition dependence. At 298°K , the slope, $\Delta\sigma/\Delta c$, is 24 Kg/mm^2 per atomic percent oxygen equivalent for Figure 5.

D. Compressive Strength Versus Grain Size

The range of grain sizes investigated is shown in Figure 7 where micrographs of the finest and coarsest grain sizes are shown. The microstructures consisted of equiaxed grains with average linear intercepts ranging from 7 to 100μ . Initially sections were taken transverse and longitudinally to determine whether there was a difference in grain shape or size. No difference was found between sections and, as a result, further samples were taken perpendicular to the compressive axis.

Figures 8, 9 and 10 summarize the results of room temperature tests performed on various grain sizes of alloys A, B and C. These results are from the alloys recrystallized at 1100°C . Listed below in Table V are the k (Hall-Petch slope) values calculated from the data. A linear regression analysis was used for analyzing the data. Two conclusions are immediately obvious: first, there is a large difference in k between alloys A and B and alloy C; second, the k values

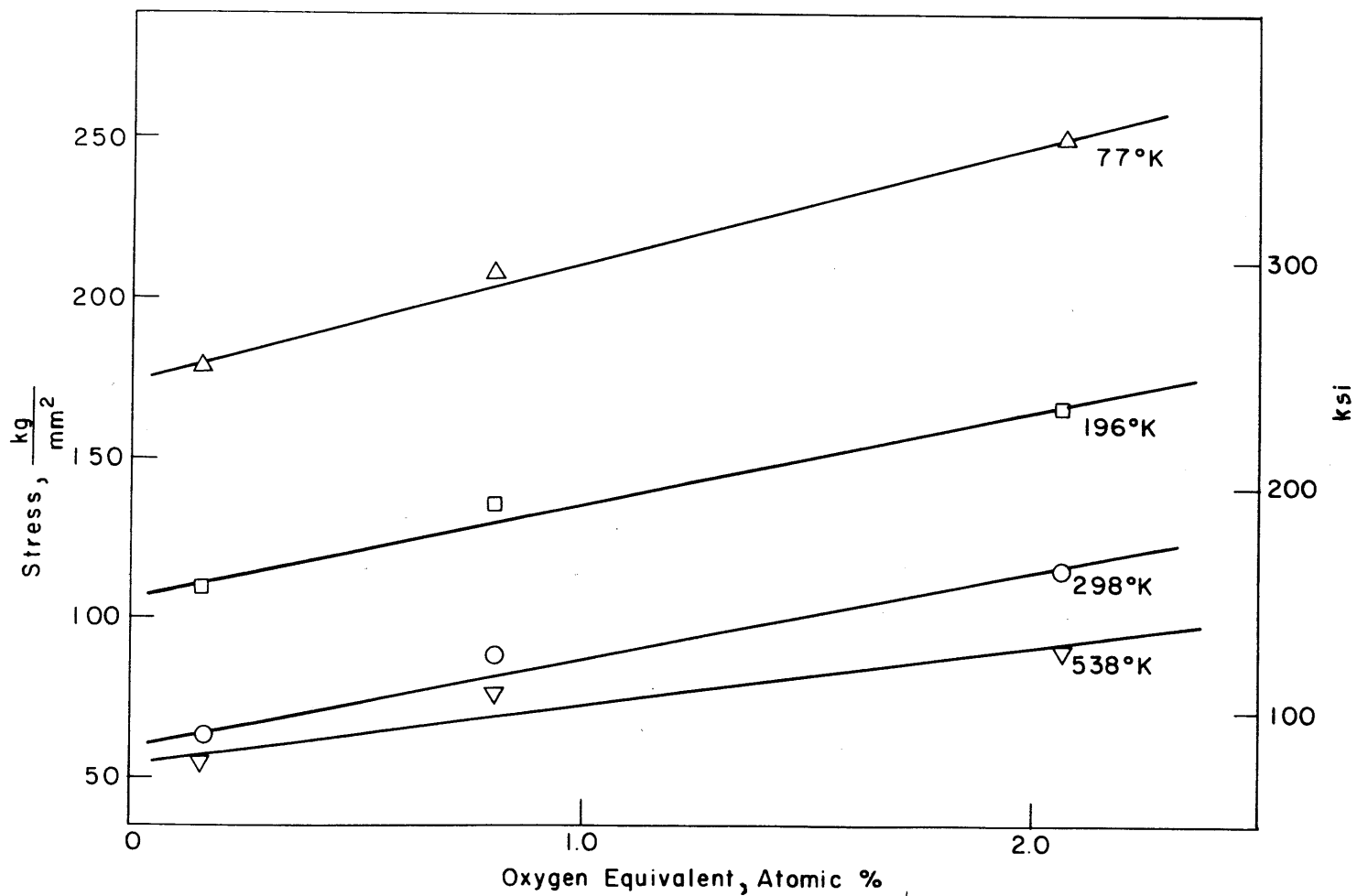


Figure 5: A plot of the yield strength of the alloys A, B and C at various temperature versus the oxygen equivalent.

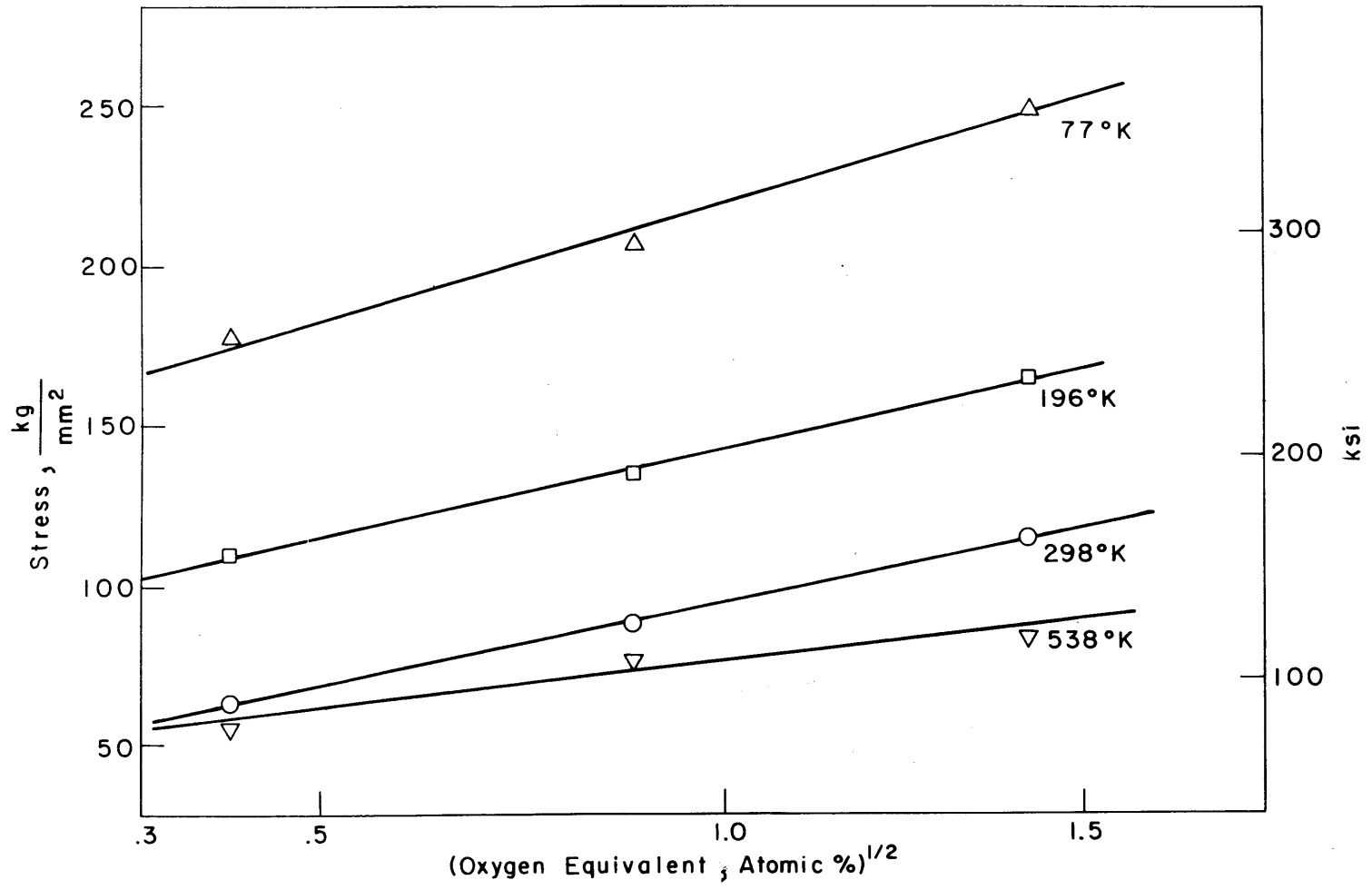
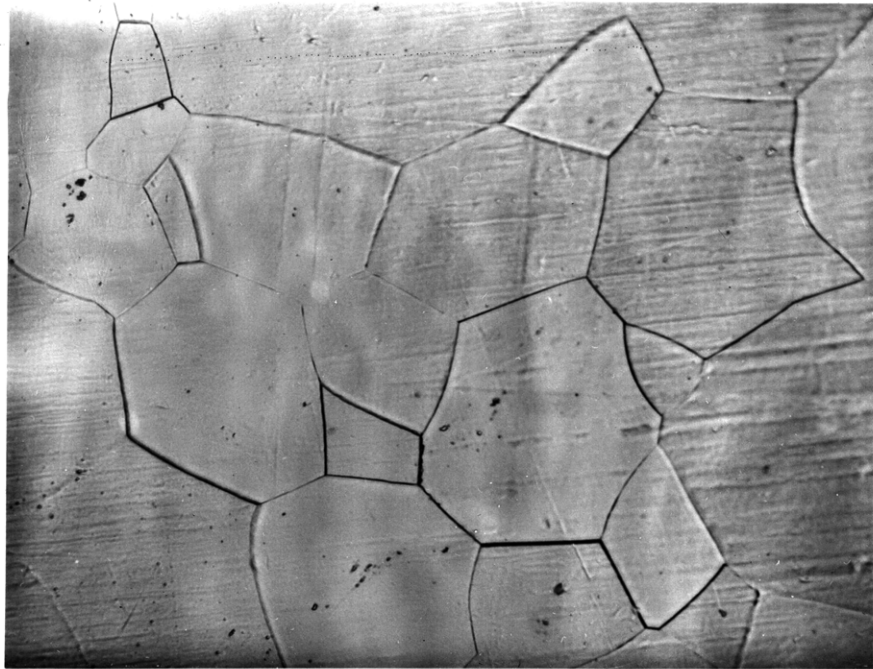


Figure 6: A plot of the yield strength of alloys A, B and C at various temperatures versus the square root of the oxygen equivalent.



(a) Grain size, 7μ .



(b) Grain size, 100μ .

Figure 7: Typical microstructures of the three titanium-molybdenum-oxygen alloys depicting the range of grain size studied. Magnification, 300X.

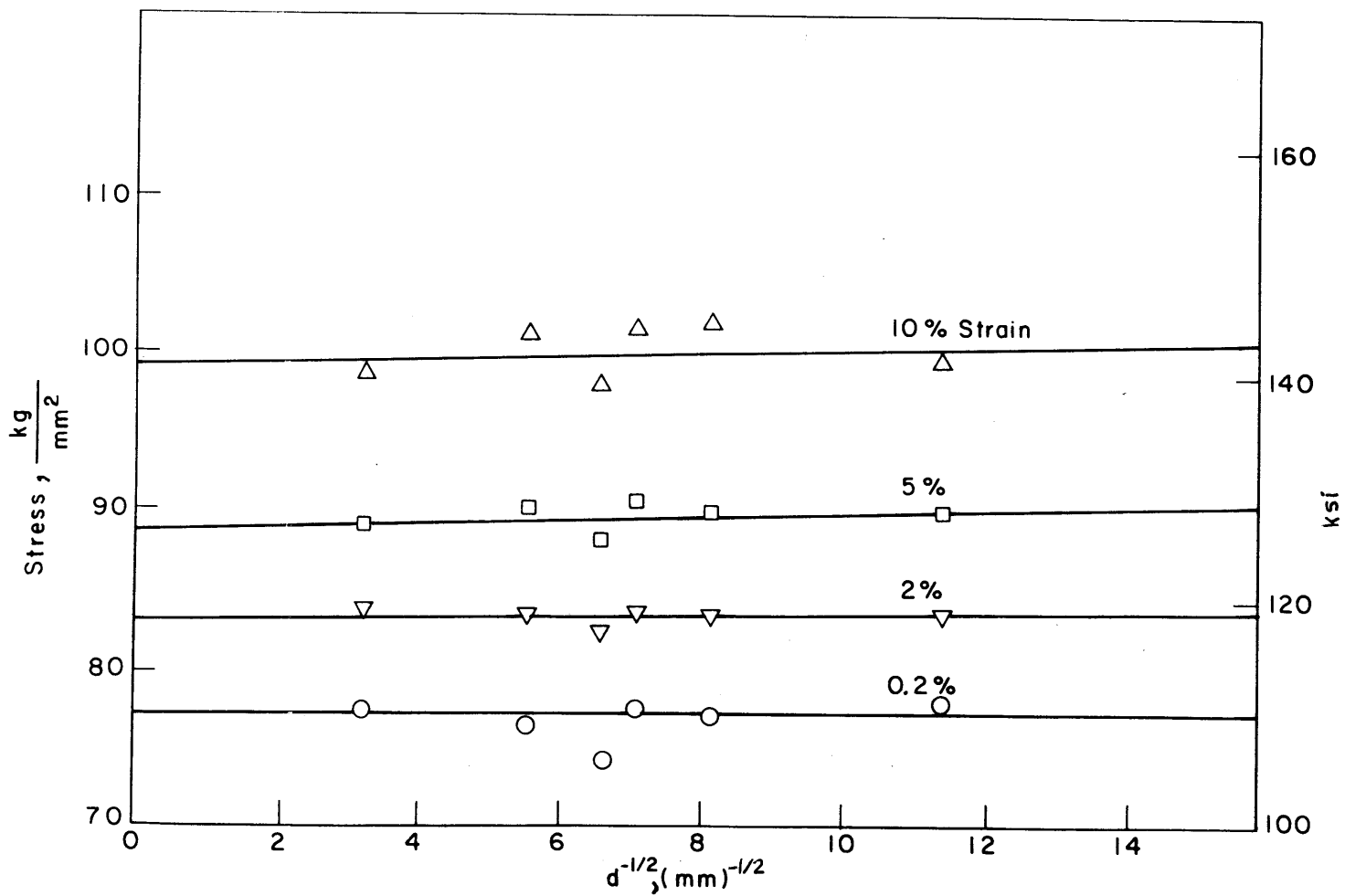


Figure 8: The yield and flow stress dependence on grain size for alloy A.

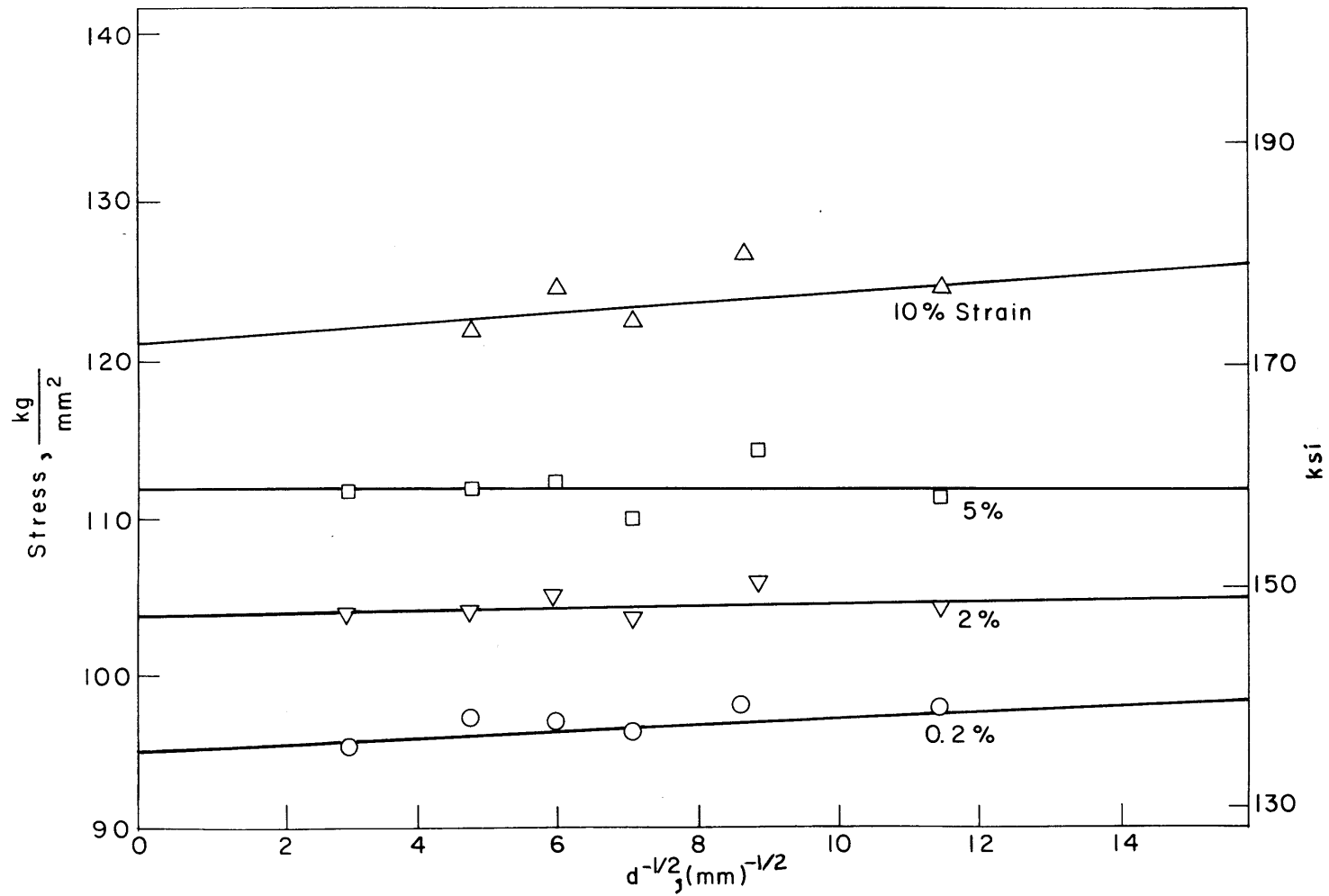


Figure 9: The yield and flow stress dependence on grain size for alloy B.

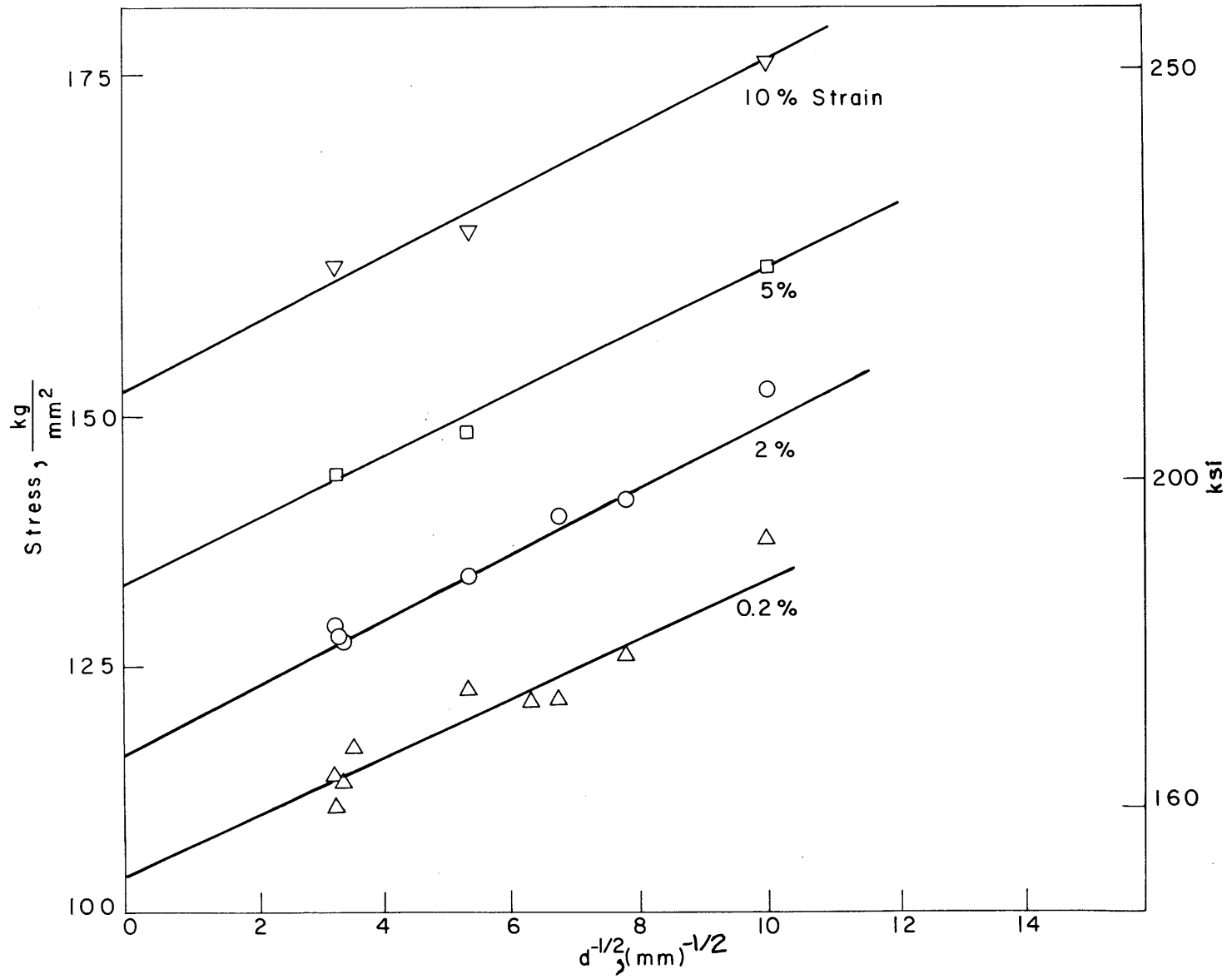


Figure 10: The yield and flow stress dependence on grain size for alloy C.

Table V

Values of k , the Hall-Petch Slope, for Alloys A, B and C at Various Strains. Recrystallization Temperature was 1100°C .

<u>alloy</u>	<u>strain</u>	<u>k, $\text{Kg/mm}^{3/2}$</u>
A	0.2	- ^a
	2.0	0.03
	5.0	0.14
	10.0	0.13
B	0.2	0.26
	2.0	0.11
	5.0	0.03
	10.0	0.41
C	0.2	2.4
	2.0	2.8
	5.0	2.7
	10.0	2.8

(a) Data too scattered for linear analysis.

change in a random way with strain. The change in k within one alloy is probably not statistically meaningful. The range of grain size covered and the accuracy of the stress determination do not lend themselves to distinguishing differences in k 's of 0.03 and 0.41. One important point, however, is that all the curves for alloys A and B do show a positive slope indicating a small but finite effect of grain size.

The results of testing samples of alloy A that had been recrystallized at 900°C are shown in Table VI below.

Table VI

Values of k for Alloy A at Various Strains.
Recrystallization Temperature was 900°C.

<u>strain</u>	<u>$\frac{k}{\text{Kg/mm}^{3/2}}$</u>
0.2	0.05
2.0	0.01
5.0	0.09
10.0	0.08

Alloy A again showed a small but measurable effect of grain size. A similar trend was noted for samples of alloy B that had been recrystallized at 900°C. It was therefore concluded that the effect of recrystallization temperature was insignificant.

Aging samples of alloys A and C for 30 minutes at 450°C also had no effect on the relative slopes of these alloys. The k value for alloy A at 0.2% offset was 0.0 Kg/mm^{3/2} based on three tests at each of three grain sizes. The alloy C results yielded a k of 2.3 Kg/mm^{3/2}. These values compare favorably with those given in Tables V and VI.

The tests performed at 77°K on alloy A also showed little effect of grain size on strength yielding a k value of slightly less than zero at 0.2% offset from limited data. This negative value is deemed not meaningful and is the result of insufficient data.

E. Electron Microscopy

1. Dislocation Structure.

Examination of foils from the three alloys revealed that the dislocation structure was the same irrespective of the oxygen content. At low strain, 0.5 percent, a few bands of dislocations were noted with the dislocations in them usually quite closely spaced. The number of bands did depend on the alloy since as shown later the density was a function of the oxygen content. A series of typical micrographs are shown in Figures 11, 12 and 13. As the strain was increased the number of bands increased while the density within a band did not. At strains of 10 and 15 percent, foils showed long straight dislocations with no evidence of cell formation. Generally three different orientations of dislocations were observed, rarely a fourth was visible. Using a $\langle 200 \rangle$ reflection would image all dislocations of $\langle 111 \rangle$ Burgers vectors.

2. Dislocation Density Measurements.

The table below lists the dislocation densities measured for alloys A, B and C at various strains. The dislocation density data is plotted as a function of strain in Figure 14 for alloys A and B, and Figure 15 for alloy C. The accuracy of the measurements was demonstrated by noting the variation in density from foil to foil. The densities at approximately four percent strain varied up to ten percent between foils with most of the variations under five percent.

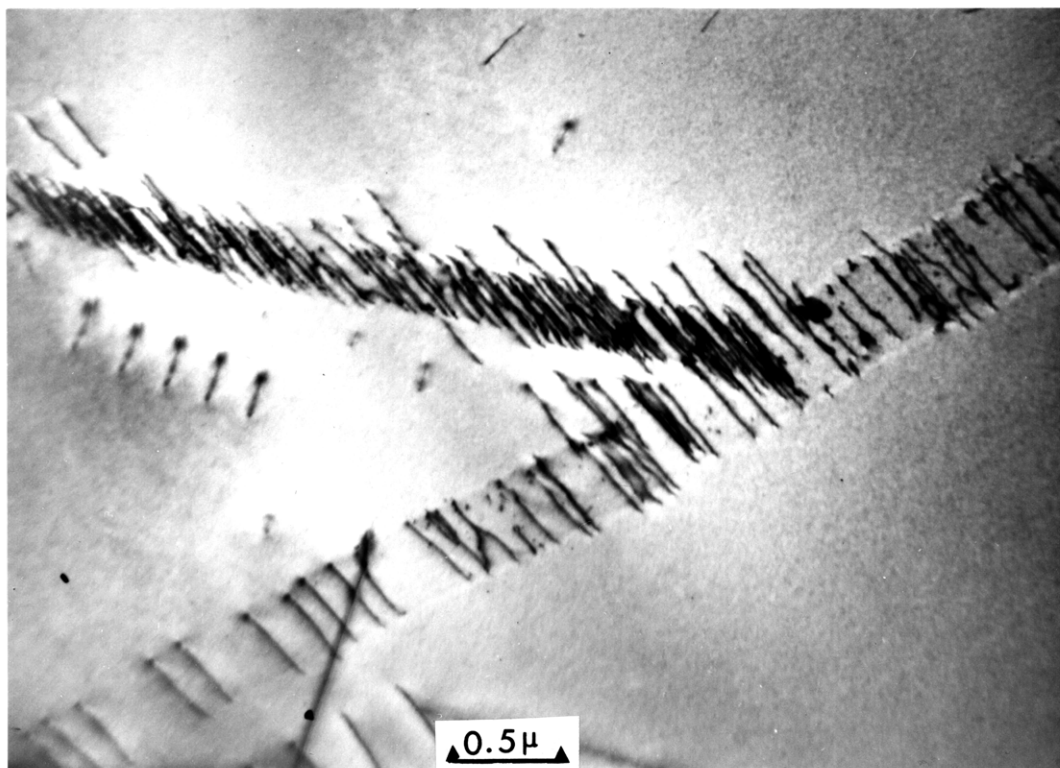
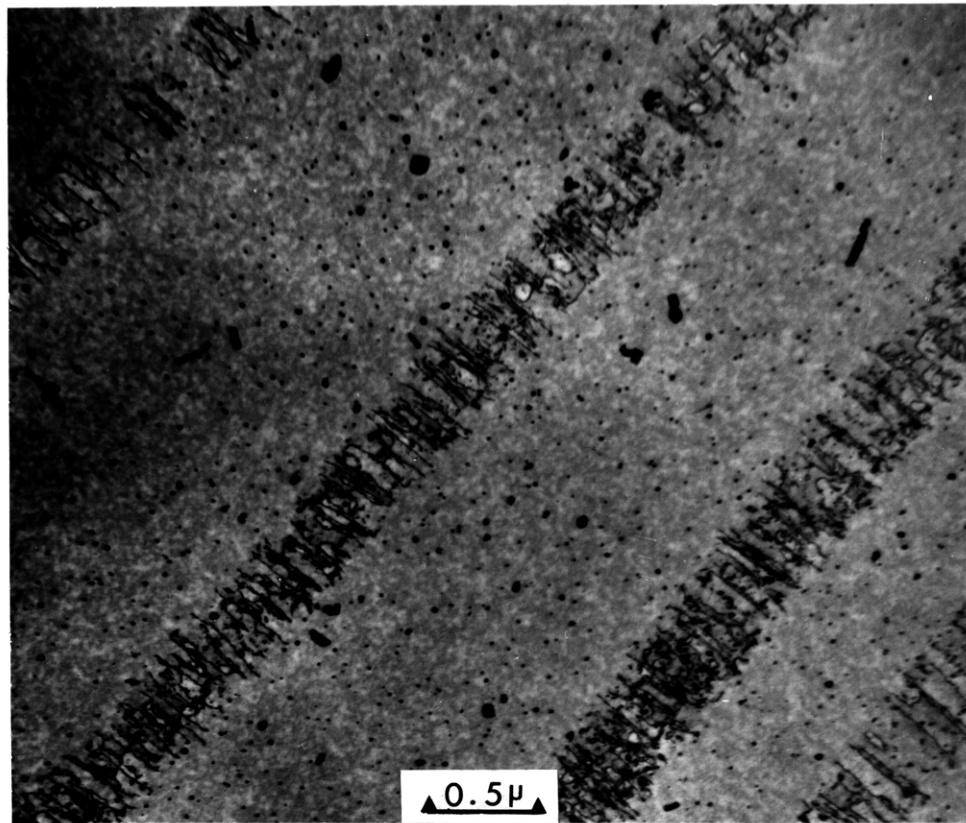


Figure 11: Two examples of dislocation structures observed at 0.5 percent strain in the titanium-molybdenum-oxygen alloys.

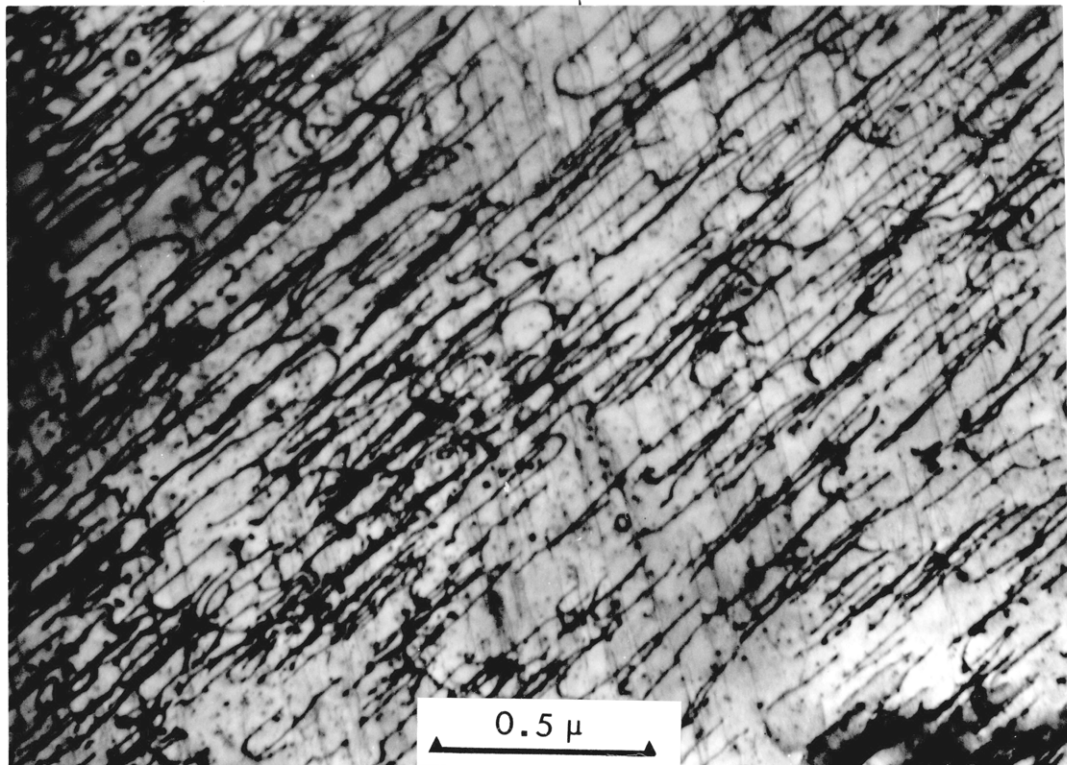
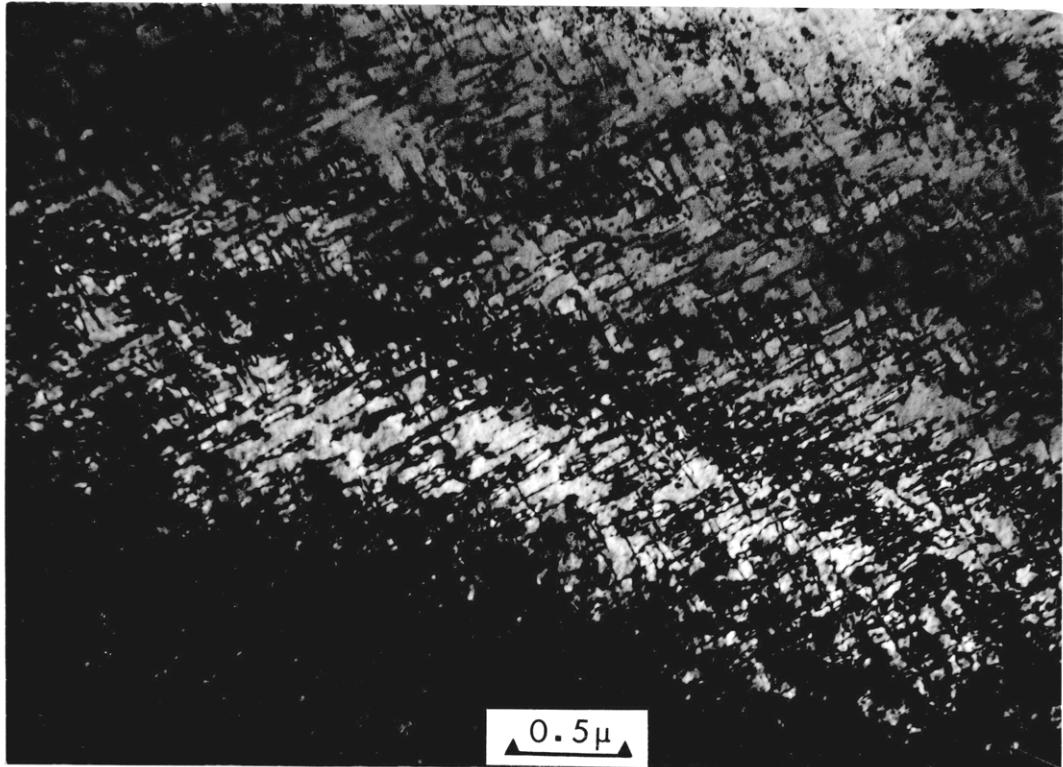


Figure 12: Two examples of dislocation structures observed at 2.0 percent strain in the titanium-molybdenum-oxygen alloys.

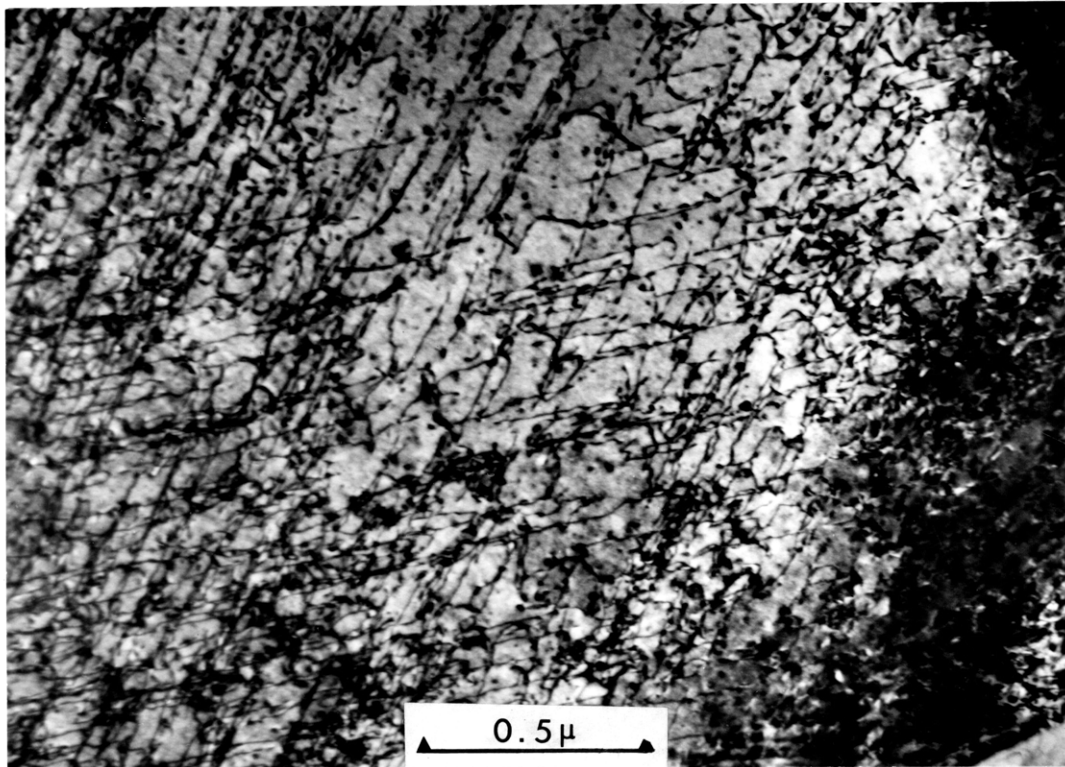


Figure 13: Typical dislocation structure observed at 4.0 percent strain in the titanium-molybdenum-oxygen alloys.

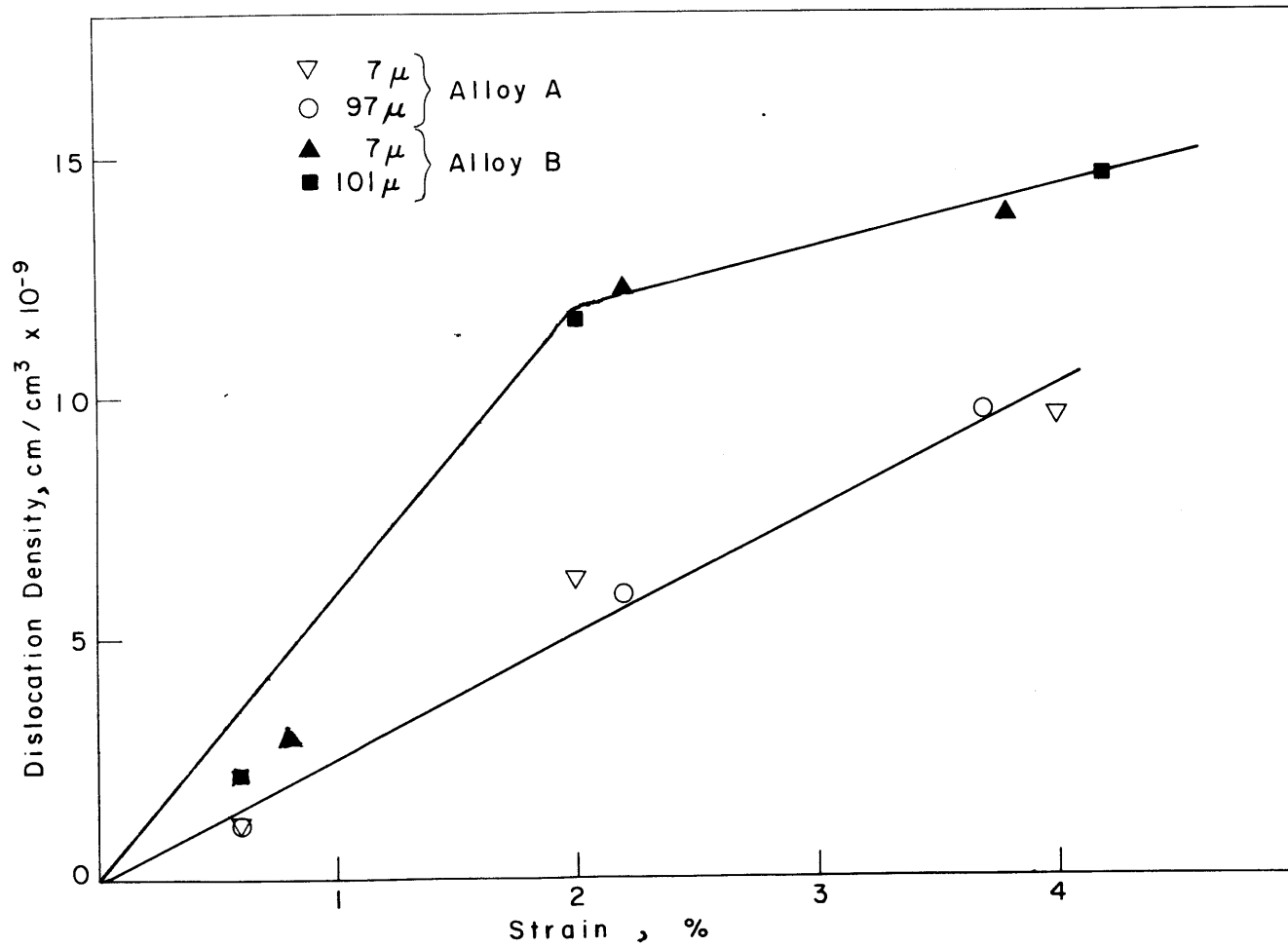


Figure 14: The effect of strain on the dislocation density for alloys A and B.

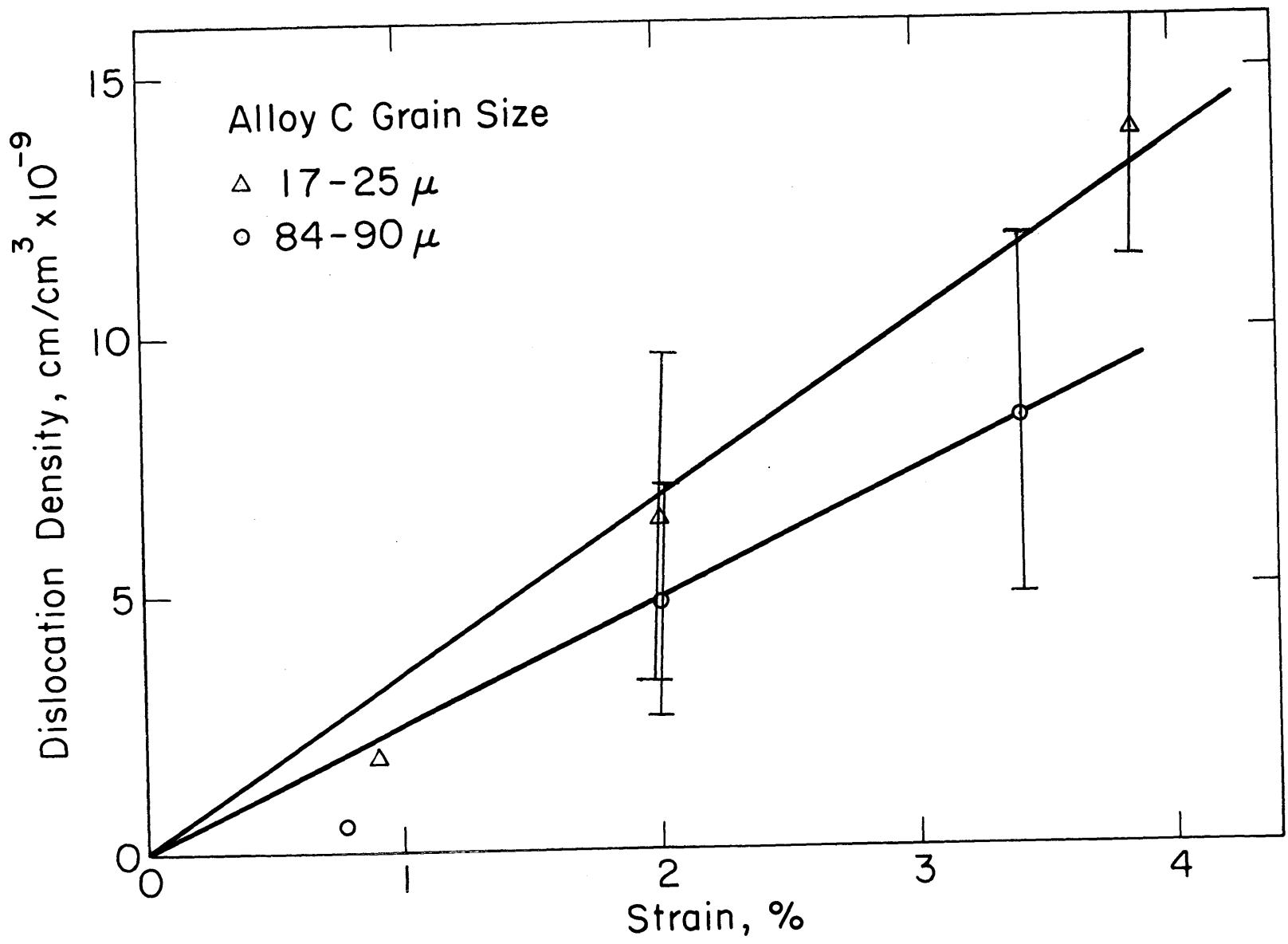


Figure 15: The effect of strain on the dislocation density for alloy C.

Table VII

Dislocation Densities of Alloys A, B and C
at Various Strains

<u>alloy</u>	<u>grain size,</u> <u>μ</u>	<u>strain,</u> <u>%</u>	<u>dislocation density,</u> <u>$\text{cm}/\text{cm}^3 \times 10^{-9}$</u>
A	7	0.6	1.1
		2.0	6.2
		4.0	9.6
A	100	0.6	1.1
		2.2	5.9
		3.7	9.7
B	7	2.2	12.3
		3.8	13.9
B	101	2.0	11.6
		4.2	14.6
C	25	0.9	1.8
	17	2.1	6.4
	22	3.8	13.9
C	90	0.8	0.5
	88	2.0	4.8
	84	3.4	8.3

As the amount of strain decreased the foil-to-foil variation increased. At 0.5 percent strain, the variation from foil-to-foil was as much as 50 to 100 percent while for the 2 percent strained samples the variation averaged 21 percent from foil-to-foil. In addition, the alloy C data for 2 and 4 percent strain is shown with error limits representing \pm two standard deviations. The first point in the figures to note is that there is no difference in density as a function of strain between 7 and 100 μ grain size for alloys A and B. Alloy C on the other hand does show a dependence on grain size as well as strain

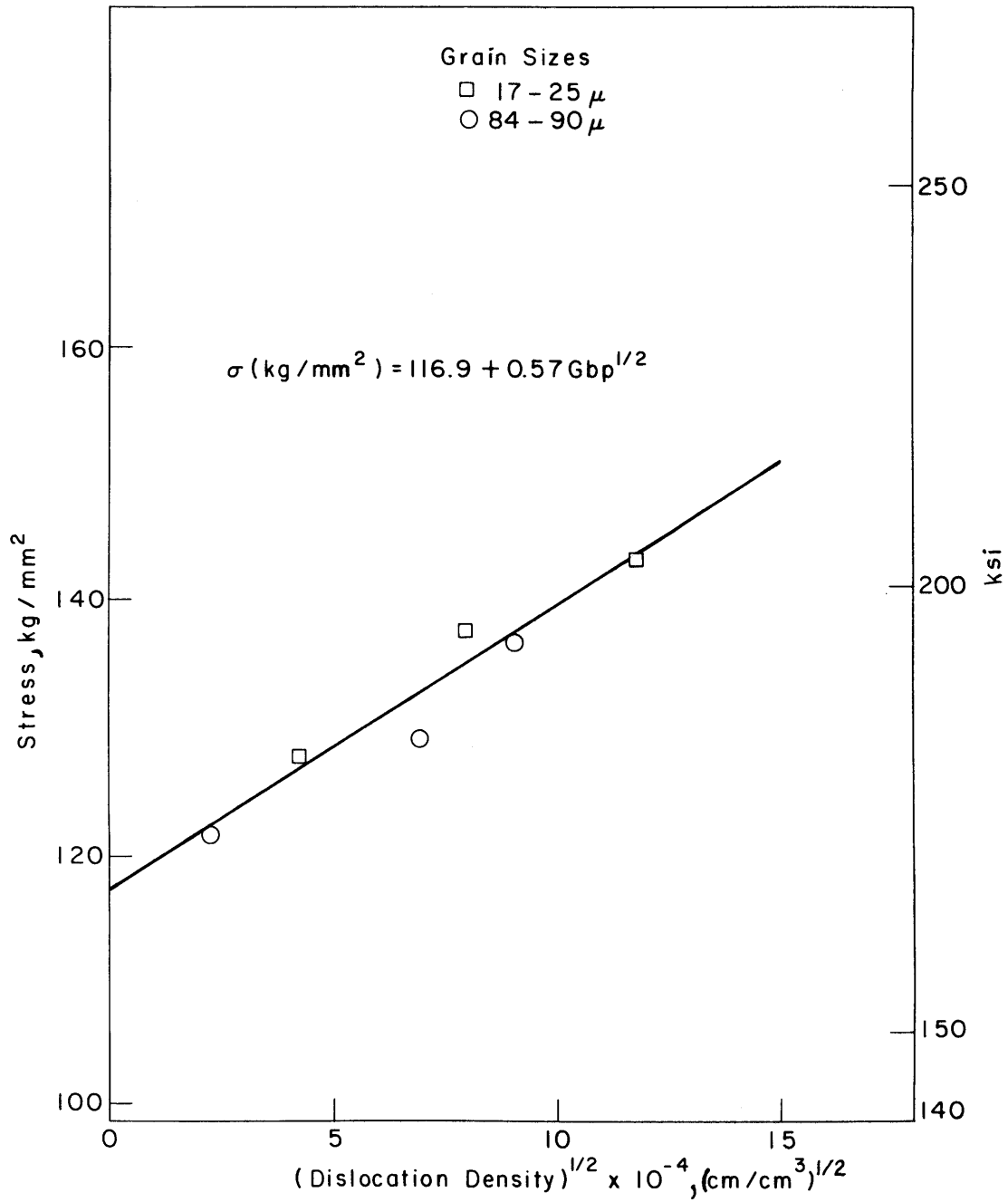


Figure 16: Flow stress versus the square of dislocation density for alloy C.

for dislocation density. The other point to note is that the density of alloy B is greater than that of alloy C at comparable strains and that at low strains the density of alloy A is greater than either grain size of alloy C.

Figure 16 shows the data for both grain sizes plotted as a function of stress versus the (dislocation density)^{1/2}. The equation associated with this type of plot is: $\sigma = \sigma_0 + \alpha Gb\rho^{1/2}$ where σ_0 is termed the friction stress, α a numerical factor, G the shear modulus and b the Burgers vector. The factor α was found to have a value of 0.57.

3. Slip Plane Determinations.

Slip plane determinations done on the alloys at all strains revealed the (211). In at least two cases the line along which the slip plane pole lay intersected both (211) and (110) planes. Using the fact that the $\langle 111 \rangle$ direction was perpendicular to the direction always eliminated the (110) and yielded the (211) plane 90° from the $\langle 111 \rangle$. The (123) plane which is sometimes observed in b.c.c. metals was only near the trace once and in that case the $\langle 111 \rangle$ direction again eliminated it.

4. Burgers Vector Determination.

The Burgers vector was assumed to be $\langle 111 \rangle$ at the outset. The use of the $g \cdot b = 0$ criterion proved this assumption to be correct and also showed that the dislocations in the bands were of screw type.

V. DISCUSSION

A. Lattice Constant Determination

The lattice constant increase measured for titanium-30 weight percent molybdenum was 0.0063 Å per atom percent oxygen. This increase is nearly comparable with the value of 0.0045 Å per atom percent oxygen found for tantalum(58). The titanium-molybdenum lattice constant increase is of the right magnitude relative to tantalum if one assumes that in both metals the oxygen tetravalent radius is the same and the octahedral position is the site occupied. Further, tantalum has the larger lattice constant and hence would suffer less lattice distortion when oxygen is added. An observed linear increase in the lattice constant shows that oxygen is in solution up to the highest amount studied, approximately 2 atom percent. Further, the solubility of oxygen in titanium-30 molybdenum has been shown to be 3.5 atom percent at 1100°C(1), the solution annealing temperature in this work.

B. Comparison of Tension and Compression Tests

Previous work on martensitic ferrous alloys(59) found that the yield strength measured in compression was significantly greater than that found in tension. One rationalization of this effect had been in terms of non-linear elastic interactions between dislocations and interstitial solute atoms(60), while other explanations

involve microstructural characteristics of martensite. One of the original aims of the present work was to investigate the strength-differential effect in titanium-molybdenum where the results would not be complicated by the influence of residual stresses, microcracks, and retained austenite typically found in quenched martensite. Two possibilities to explain the absence of a strength-differential (Table IV) are: (1) the strength-differential effect is characteristic of martensitic alloys only or, (2) since the amount of interstitial strengthening observed in titanium-molybdenum is much less than found for carbon in iron and the solute-dislocation interaction is correspondingly weaker, the sensitivity of the present experiment was not sufficient to detect this effect. One cannot differentiate between these two possibilities from the results of the present investigation.

C. Yield Strength Versus Temperature

As noted earlier in the literature review, the effect of interstitial solute above a concentration in excess of 500 parts per million is athermal in nature. The observed variation of yield strength with temperature for the three beta phase alloys studied in this work (Figure 3) indicates that the effect of oxygen on titanium-30 molybdenum is indeed athermal in nature. The range of interstitial content studied included 320 to 5000 ppm. The increase in yield strength with temperature is typical of b.c.c. metals

and is equal in magnitude to the observations of Zeyfang and Conrad for a titanium-26.4 molybdenum alloy containing 0.5 atom percent oxygen equivalent(3).

The general shape of the stress-strain curves shown in Figure 4 is similar to those reported by Pugh for molybdenum(61), Conrad for titanium-26 molybdenum(3) and other b.c.c. metals. The rate of work hardening for the present alloys is also similar to that found in the forenamed molybdenum and titanium-26 molybdenum.

One characteristic of flow curves from interstitially strengthened b.c.c. metals lacking in the alloys studied in this work is a yield point. As noted earlier, even aging treatments failed to produce a noticeable yield point in both alloys A and C. A theory for the yield point was developed by Hahn(62) utilizing the dislocation dynamics of Johnston and Gilman(63). According to this approach, the dislocation velocity is stress dependent or,

$$v = \left(\frac{\sigma}{\sigma_0}\right)^m \quad (16)$$

where v is the dislocation velocity, σ is the applied stress, σ_0 is the stress for unit dislocation velocity, and m is a numerical constant. The value of m must be small for a large yield drop to be observed. Values of m over 100 result in imperceptible yield drops. Iron, on the other hand, has an m -value of 35 and exhibits a yield point. An even greater yield point is shown by lithium fluoride where the value of

this exponent is 16.5. Another criterion for the occurrence of a yield point is a low initial mobile dislocation density. In interstitially strengthened b.c.c. metals, this requirement is easily satisfied when the interstitials form anchoring atmospheres around grown-in dislocations to lower the initial mobile dislocation density. Formby and Owen(51) showed that for tantalum-oxygen, the yield point could be eliminated by quenching from a temperature where interstitial atoms presumably did not form atmospheres around dislocations. Two possibilities exist for the lack of a yield point in b.c.c. titanium-molybdenum: (1) the dislocation velocity is very stress dependent (a high m value) and (2), dissolved oxygen is randomly distributed in the lattice and not at dislocations. The first possibility is unlikely since there is no reason to expect that titanium-molybdenum is an anomaly among b.c.c. metals. The second possibility means that strong binding exists between oxygen and titanium and/or molybdenum atoms, and that such binding forces are greater than those between oxygen and dislocations and other oxygen atoms. The fact that an ageing treatment could not induce a yield point supports the later proposal. Thus, it appears that the initial mobile density is high since the grown-in dislocations are not effectively pinned.

Data depicting the strengthening effect of oxygen in Figures 5 and 6 leave unanswered the question of a linear or square root dependence of strength upon oxygen concentration. It seems more likely that the linear

dependence is correct when compared with the results of interstitial containing vanadium(31), tantalum(23,24) and niobium(25). For these three metals, the increase in strength was found to be linear when a large range of interstitial content, usually up to one atom percent, was investigated. The strengthening increase of titanium-molybdenum, expressed as $\Delta\sigma/\Delta c$ in terms of the shear modulus, G , is $0.2G$. This value is comparable in magnitude to the values reported for the metal-oxygen systems summarized in Table I. A portion of that table and the titanium-molybdenum data are compiled in Table VIII.

Table VIII

Interstitial Strengthening of Several B.C.C. Metals

<u>system</u>	<u>$\Delta\sigma/\Delta c$</u>	<u>lattice constant, A</u>
vanadium-oxygen	0.4 G	3.030
niobium-oxygen	0.3 G	3.301
tantalum-oxygen	0.2 G	3.303
titanium-30 molybdenum-oxygen	0.2 G	3.243

The strengthening in b.c.c. metals is proportional to the lattice distortion produced by the addition of interstitial solute atoms. If one assumes that the oxygen atom resides in the octahedral position for all four metal-oxygen alloys, then the strengthening values would be inversely proportional to the lattice constant. The only exception to this premise

is the titanium-molybdenum data. The fact that titanium-molybdenum does not show a strengthening value between vanadium and niobium could be rationalized by considering the effect of molybdenum and oxygen on the lattice constant of b.c.c. titanium. Molybdenum decreases the lattice constant of titanium while the opposite effect results from oxygen additions. A pairing of molybdenum and oxygen to reduce lattice distortion would reduce the strengthening which is dependent upon the degree of lattice distortion.

The octahedral site was the position assumed to be occupied for all four metal-oxygen systems cited above since observed strengthening values and lattice constants are comparable for all the systems. As mentioned earlier, the tetrahedral site can accommodate without lattice distortion an interstitial atom twice as large as is possible in the octahedral site. If different interstitial sites were occupied in the various alloys, a marked difference in strengthening would be observed as a consequence of the differing lattice distortion. The conclusion that the same site is occupied in all four metals contradicts Beshers(29) work where oxygen is predicted to be found in the octahedral site in vanadium and in the tetrahedral site in tantalum and niobium.

D. Grain Size Effects

One result which particularly warrants discussion is the value of the Hall-Petch-slope (k) found for alloys A and B. As shown in Tables V and VI, the values of k vary from 0.01 to 0.41 $\text{Kg/mm}^{3/2}$. In addition, these values do not vary in any systematic manner with strain. In many metals, the value of k_y is greater than k_f , but in many instances the two constants are equal. In addition, some values of k_f are greater than k_y in a metal. Meakin and Petch(39) have related the change in the value of k to the dislocation structure. For those metals where cross slip is possible k_f values are lower than k_y values. Meakin and Petch reasoned that as a cell structure forms as the result of cross slip, the limiting barrier to dislocation motion is no longer the grain boundary but the cell walls which develop. When cross slip is not possible and dislocations remain confined to their slip plane, the value of k_f might be equal to or greater than that of k_y . With the exception of the k value of 0.41 $\text{Kg/mm}^{3/2}$ for alloy B, the k values in Table V for alloys A and B are in effect equal within the experimental error inherent in determining the flow stresses. For example, a value of k equal to 0.25 $\text{Kg/mm}^{3/2}$ represents a change in strength of only 1.75 Kg/mm^2 over the range of grain sizes investigated. The estimated experimental error of ± 2 percent in determining the flow stress is equivalent to at least 1.5 Kg/mm^2 . Thus, it is

difficult to differentiate between k values of 0.03 and 0.26. The relevant result from alloys A and B is that the values of k are positive and equal and that the influence of grain boundaries on strength is small.

Alloy C is also found to have k_y and k_f values of comparable magnitude (Table V). The value of $2.4 \text{ Kg/mm}^{3/2}$ for k_y and 2.7 and 2.8 $\text{Kg/mm}^{3/2}$ for k_f are, as indicated earlier, within the experimental error of determining the flow stress, and are thus in effect comparable values. The important results are that alloys A and B show a small, almost negligible influence of grain size on strength while alloy C shows an appreciable effect, and that for each alloy, the values of k_y and k_f are comparable. For alloy C, the grain size dependence is also significant relative to other b.c.c. metals as shown by comparison with the values of k_y given in Table II. As stated above, Meakin and Petch concluded that dislocations which remain confined to their slip plane result in values of k_f equal to or greater than k_y values. The microstructure observed in all three titanium-molybdenum alloys consisted of dislocations confined to (211) planes and aligned in definite slip bands (Figures 11, 12 and 13). Thus, the fact that the values of k_y are the same or less than the values of k_f for alloys A, B and C agrees with the Meakin and Petch conclusion concerning the change in the value of k as related to microstructure.

It has been shown that for alloys A and B, the grain boundaries contribute a negligible strengthening effect while alloy C exhibits considerable grain boundary strengthening. The work hardening model would predict that for alloys A and B, the dislocation density would not be a function of grain size. This is precisely the case as shown by Figure 14, where the data for two extremes of grain size (7 and 100 μ) fall on the same curve of dislocation density versus strain for each alloy. On the other hand, the data for alloy C (Figure 15) shows that the dislocation density is a function of grain size in this alloy. Here, two different linear dependences of density upon strain are shown for grain size ranges of 17 to 25 μ and 84 to 90 μ .

The work hardening model discussed earlier can be used to explain the observed influence of grain boundaries on strength. According to this model, one can relate the flow stress to the dislocation density through equation (6),

$$\sigma = \sigma_i + \alpha G b \rho^{1/2} \quad (6)$$

Figure 16 shows the dislocation density for alloy C plotted as a function of flow stress. The application of equation (6) to the data for alloy C is quite good. The numerical constant, α , is found to have a value of 0.5 which is typical for b.c.c. metals. Conrad(64) reports a range of α values for b.c.c. metals from 0.07 to 0.67 with a typical value of 0.43 for vanadium, 0.07 to 0.34 for tantalum and 0.53 to 0.67 for niobium. Values of the friction stress, σ_i calculated from

equation (6) can be compared with the comparable stress term in the Hall-Petch relation as an additional test for the validity of equation (6). The friction stress determined from equation (6) is 117 Kg/mm^2 , while the Hall-Petch relation yields a friction stress of 107 Kg/mm^2 . The agreement is reasonable.

Before attempting to explain the grain boundary strengthening results, it is important to consider what one might expect to observe with respect to the dislocation density as a function of oxygen content. It has been shown that addition of oxygen to titanium-molybdenum considerably raises the yield strength while the characteristic appearance of the dislocation structure is not effected. Both Conrad(65) and Keh(66) have measured the dislocation density in metals as a function of the magnitude of the yield strength. In Conrad's case, the strength of α -titanium was raised through the addition of impurities while Keh, working with iron, employed the effect of temperature on the yield strength to induce a change in stress. In both iron and α -titanium, it was observed that as the stress level is raised, the dislocation density at an equivalent strain also increases. Thus, three differing curves of dislocation density versus strain are expected for the titanium-molybdenum-oxygen alloys studied here. Alloy A should exhibit the lowest dislocation density at equivalent grain size while alloy C should contain the highest density. In addition, the curves are expected to

have comparable slope as observed in iron by Keh. Keh used sufficiently low temperatures to effect a change in yield stress without appreciably changing the appearance of the dislocation structure. Conrad, on the other hand, found differing slopes for plots of dislocation density versus strain, but his result was influenced by differing dislocation structures. Based upon past results, one can expect to find curves which look schematically like Figure 4 with stress replaced by dislocation density for the three titanium-molybdenum-oxygen alloys considered in this work. The curves should exhibit comparable variation of dislocation density with strain, but with the curves displaced to higher levels of dislocation density with added oxygen content. This trend however, is not observed. Instead only two alloys, A and B, exhibit such behavior where B shows a higher dislocation density at a given strain as compared to alloy A and the slopes are comparable. Alloy C, surprisingly, exhibits a dislocation density comparable to alloy A for all strains.

The fact that alloy C does not exhibit a higher dislocation density than alloys A and B, at a given strain, will now be related to the average slip distance, $\tilde{\lambda}$, for dislocation motion. The total dislocation density is related to $\tilde{\lambda}$ through equation (8),

$$\epsilon = \rho b \tilde{\lambda} \quad (8)$$

where ρ is the total density of dislocations which have contributed to the strain. It is obvious that a decrease in the mean slip length must be associated with a comparable increase in dislocation density to accommodate the imposed plastic strain. As mentioned earlier, Kocks(42) has stated that this mean slip length is inversely proportional to the applied stress. For this to be true, alloy C, which possesses the highest yield strength, should be characterized as having the shortest slip distance and therefore, the highest dislocation density at a given strain. However, it was found in this study that this alloy having the highest strength exhibited an unexpected low dislocation density, below that found for alloy B.

It is worthwhile to summarize the results up to this point in order to clarify what is to follow. Alloys A and B exhibit dislocation densities which are not dependent upon grain size. As the oxygen content increases for alloys A and B, the dislocation density at equivalent strains increases. One must conclude from these last two statements that oxygen is interacting with dislocations to form a barrier which is controlling the dislocation slip length. Only in alloy C is the dislocation density variable with grain size. The conclusion which evolves is that grain boundaries contribute to strengthening only when they act as controlling barriers to dislocation motion, as in alloy C. When a barrier of smaller dimensions than the grain diameter exists, the strengthening effect of grain boundaries will be substantially

reduced, as in alloys A and B. In other words, the barrier to dislocation motion in alloy C is the grain boundary while some other barrier exists in alloys A and B, in addition to the grain boundary.

The interaction proposed above serves to limit the average slip distance to a value much less than the grain diameter. As a result, in alloys A and B, the grain boundary is not the factor controlling the level of strength in that the dislocation density is determined by the oxygen content through its effect on the average slip distance. The mean slip distance decreases with increasing oxygen content with resultant higher dislocation density.

Interstitially dissolved oxygen serves to form a barrier to slip within a grain. This is evident when one bears in mind the work of Formby and Owen(51). These workers were able to change the value of k_y from zero to $2.1 \text{ Kg/mm}^{3/2}$ by varying the heat treating temperature. A high value for k_y resulted when oxygen was redistributed to form atmospheres around dislocations with a resultant increase of the mean slip distance to an extent approximating the grain diameter. A low value for k_y resulted when the alloy was quenched from a temperature where the oxygen was completely in solution. When in solution, oxygen acts as a barrier to dislocation motion through interaction of its strain field with that of dislocations.

The value for k_y can also be varied in iron-carbon alloys by various quenching and ageing treatments, as shown by Fisher(67), when the material was tested at 77°K where no ageing reactions could complicate the results. The quenched samples yielded lower values for k_y when compared to the values of k_y obtained for ageing. The observed variation in the value for k_y in iron was not as dramatic as noted in tantalum. The change of $0.3 \text{ Kg/mm}^{3/2}$ in k_y was due to the low carbon content of 0.001 percent. Since the dissolved carbon barriers are more widely spaced, a less dramatic change in the value of k_y results. From the two cases cited above, it is evident that when the matrix has interstitial solute atoms distributed randomly and not around dislocations, the value of the Hall-Petch slope is reduced.

It is not possible to change the value of the Hall-Petch slope nor is it possible to develop a yield point with heat treatment in the titanium-molybdenum-oxygen alloys investigated in this work. This fact means that it is not possible in this system to redistribute interstitially dissolved oxygen between the lattice and regions around dislocations. The reason for this relative immobility of oxygen is that there exists a strong chemical as well as lattice strain interaction between molybdenum and oxygen. The lattice strain component arises since molybdenum decreases the lattice constant of beta-titanium, while oxygen dilates the lattice in an opposite but not equal sense. Thus, the

barriers to dislocation motion in the present case are randomly dispersed molybdenum-oxygen pairs or clusters. According to Tyson(6), the breaking of chemical bonds in the dislocation core may be a significant source of strengthening in titanium-oxygen alloys. The absence of a yield point in titanium-molybdenum is a consequence of the fact that atmospheres of oxygen do not form around dislocations to limit the mobile dislocation density. The interaction energies in systems where such dislocation pinning occurs is in the vicinity of 0.45 - 0.75 eV(7,51). The suggestion here is that the total interaction energy between molybdenum and oxygen exceeds the value for the interaction energy between oxygen and dislocations.

It has been shown above that interstitially dissolved solute atoms randomly distributed result in a negligible influence of grain boundaries on strength as in alloys A and B. Conversely, a larger, finite value for the Hall-Petch slope is developed when the mean slip distance for dislocations is increased from a value related to the solute spacing to a value approximating the grain diameter. This is accomplished in the tantalum-oxygen and iron-carbon alloys discussed above by ageing to redistribute the interstitial atoms from the matrix to atmospheres around dislocations. It has been shown that such redistribution is not possible in the titanium-molybdenum-oxygen alloys considered in this work. The large, finite value for the

Hall-Petch slope observed in alloy C is the consequence of the oxygen-molybdenum pairs or clusters no longer being viable barriers due to the high imposed stress at which this alloy deforms.

A schematic diagram of what is believed to be occurring in the three titanium-molybdenum-oxygen alloys considered in this work is shown in Figure 17. The curves for alloys A and B show little dependence of strength upon grain size. Increasing the oxygen content displaces the curves to higher stresses. Above a stress level equivalent to the applied stress necessary to surmount the barrier to slip provided by randomly dispersed interstitial atoms, a significant dependence of strength upon grain size is observed. Thus, below the level of stress denoted by σ_{internal} , the slip distance is limited by the barrier formed by the interaction of interstitially dissolved solute atoms and dislocations. Above this stress, the slip distance is limited by the grain diameter since the strength level is now sufficient for the applied force on dislocations to easily overcome the barrier posed by the dispersed solutes. Extrapolating to lower stresses (coarser grain sizes), it is conceivable that a value below σ_{internal} will be attained and that the grain size dependence will vanish for alloy C. This occurrence could not be verified in this case since attempts to obtain grain sizes greater than 200μ in diameter by prolonged annealing resulted

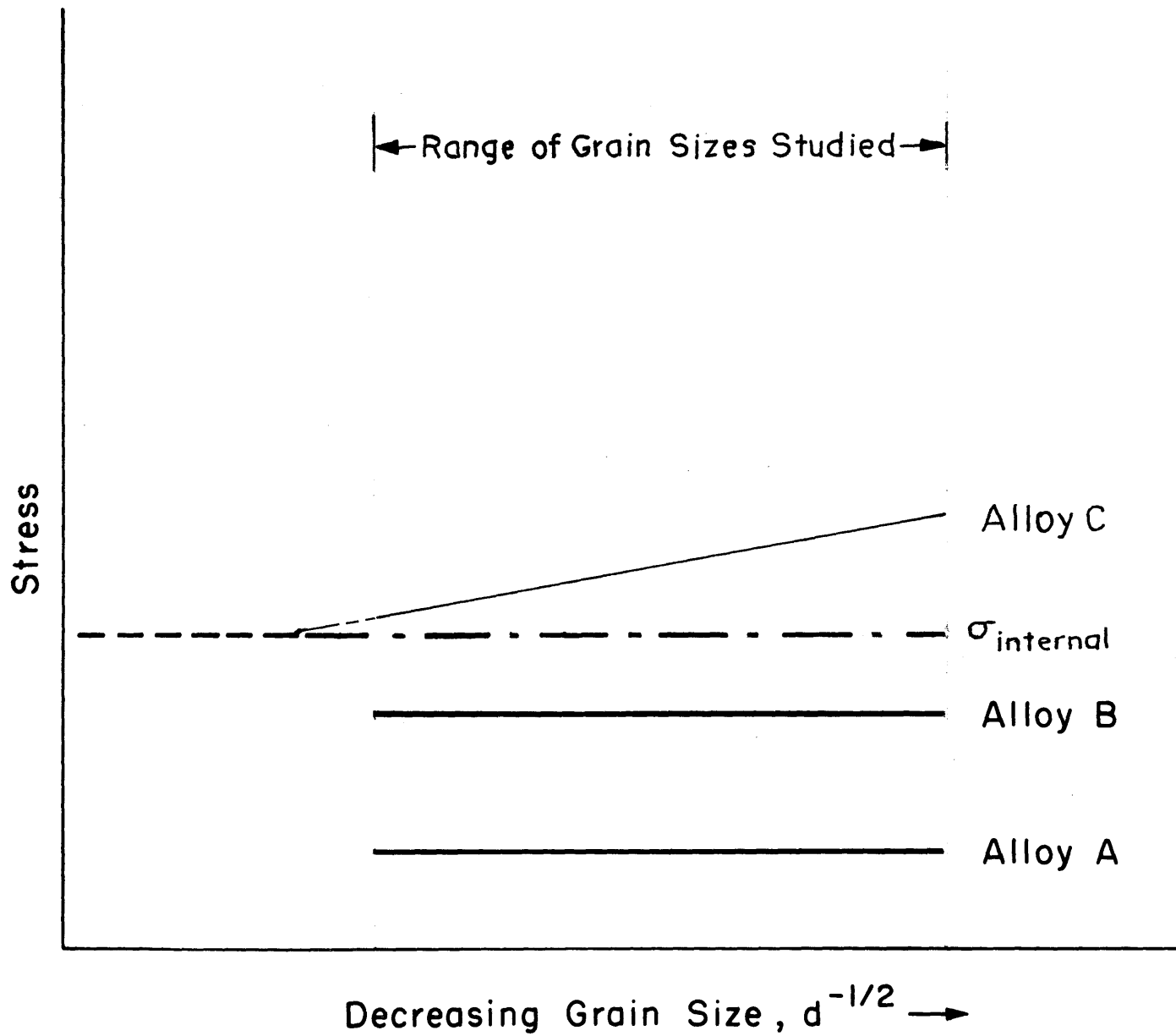


Figure 17: Schematic diagram of the effect of an internal barrier on the grain size versus stress results.

in the formation of α -titanium at grain boundaries. Attempts to reduce the grain size of alloys A and B below 7μ were also unsuccessful because of incomplete recrystallization. A more fruitful approach would be to study an alloy of oxygen content between that of alloys B and C.

VI. CONCLUSIONS

1. Oxygen produces a linear lattice constant increase up to at least 2.06 atom percent equivalent in this alloy.
2. The effect of oxygen, in the range 0.16 to 2.06 atom percent equivalent, on the flow strength at various temperatures is athermal.
3. The increase in strength at all temperatures is linear with oxygen equivalent.
4. Large values for the Hall-Petch slope are related to increased dislocation density with decreased grain size.
5. The flow stress is related to the dislocation density through the work hardening equation,

$$\sigma = \sigma_i + \alpha G b \rho^{1/2}$$

6. Small or zero values for the Hall-Petch slope yield dislocation densities which are not a function of grain size at comparable strains.
7. The absence of grain boundary strengthening is associated with an average slip length limited to less than the grain diameter. This restricted slip length is the consequence of interactions between interstitial atoms and dislocations.
8. At levels of applied stress sufficient to surmount the internal barrier, the average slip distance is limited by the grain boundary. As a result, grain boundary strengthening is possible.

VII. SUGGESTIONS FOR FURTHER WORK

1. Investigation of a wider range of grain sizes of all three alloys could confirm further the conclusions of this work. Further extension could serve to identify the strength level at which a grain size dependence is observed and aid in determining the nature of the internal barrier proposed. It should be emphasized however, that considerable difficulty was encountered developing grain sizes both finer and larger than the range studied in the work.
2. The investigation of titanium-30 weight percent molybdenum alloys with oxygen contents between alloys B and C would also aid in determining the strength level of the barrier.
3. An investigation of dislocation density and grain size dependence should be undertaken in other interstitially strengthened b.c.c. metals. In particular, those b.c.c. metals which exhibit a Hall-Petch slope which can be changed from zero to 2 or 3 Kg/mm^{3/2} should be most illuminating. This work would enable one to determine the applicability of the internal barrier proposed and of a work hardening theory to explain grain boundary strengthening.
4. An ultrapure titanium-30 weight percent molybdenum alloy investigated with respect to the grain size dependence on strength would serve to establish the interstitial as the responsible element in the internal barrier.

REFERENCES

1. P. A. Farrar, L. P. Stone and H. Margolin, *J. Metals* 8, 595 (1965).
2. F. C. Holden, H. R. Ogden and R. I. Jaffee, *J. Metals* 8, 1388 (1956).
3. R. Zeyfang and H. Conrad, *Acta Met.* 19, 985 (1971).
4. H. Conrad, *Canad. J. Phys.* 45, 581 (1967).
5. W. R. Tyson, *Canad. Met. Quart.* 6, 301 (1968).
6. W. R. Tyson, *Scripta Met.* 3, 917 (1969).
7. A. W. Cochardt, G. S. Schoek and H. Wiedersich, *Acta Met.* 3, 533 (1955).
8. J. W. Christian, *Second Int'l Conf. on Str. of Met. and Alloys, Conf. Proc. ASM* (1970).
9. K. V. Ravi and R. Gibala, *Acta Met.* 18, 623 (1970).
10. C. N. Reid, A. Gilbert, and G. T. Hahn, *Acta Met.* 14, 975 (1966).
11. L. Kaun, A. Luft, J. Richter and D. Schulze, *Phys. Stat. Sol.* 26, 485 (1968).
12. N. E. Paton and J. C. Williams, ref. 8, p. 108.
13. M. K. Koul, Ph.D. Thesis, M.I.T. (1968).
14. R. A. Foxall and C. D. Statham, *Acta Met.* 18, 1147 (1970).
15. D. S. Gelles, Ph.D. Thesis, M.I.T. (1971).
16. A. Crackell and N. J. Petch, *Acta Met.* 3, 186 (1955).
17. J. Helsop and N. J. Petch, *Phil. Mag.* 1, 866 (1956).
18. J. Friedel, *Elec. Microscopy and Strength of Crystals*, ed., G. Thomas and J. Washburn (1963), N. Y., Interscience.
19. J. Friedel, *Relation of Structure to Mechanical Properties of Metals* (1963), No. 15, London HMSO.

20. R. L. Fleischer, Acta Met. 10, 835 (1962).
21. J. Snoek, Physics 8, 711 (1941).
22. G. Schoek, and A. Seeger, Acta Met. 7, 469 (1950).
23. R. Lachenmann and H. Schutz, Scripta Met. 4, 709 (1970).
24. J. Pühr-Westerheide and G. Elssner, J. Less Common Metals 20, 371 (1970).
25. G. Elssner and G. Horz, J. Less Common Metals 21, 451 (1970).
26. K. V. Ravi and R. Gibala, Acta Met. 18, 623 (1970).
27. C. Wert, J. Metals 2, 1242 (1950).
28. W. S. Owen and M. J. Roberts, Dislocation Dynamics, p. 357, McGraw-Hill, New York (1963).
29. D. N. Beshers, J. Appl. Phys. 36, 290 (1965).
30. E. O. Hall, Proc. Phy. Soc. London B64, 747 (1951).
31. N. J. Petch, J. Iron Steel Inst. 174, 25 (1953).
32. Invited papers from Symposium on Deformation and Strength of Polycrystals, Met. Trans. 1, 1095 (1970).
33. J. C. M. Li and Y. T. Chou, Met. Trans. 1, 1145 (1970).
34. J. D. Eshelby, F. C. Frank and F. R. Nabarro, Phil. Mag. 42, 351 (1951).
35. Y. T. Chou, J. Appl. Phys. 38, 2080 (1967).
36. G. Leibfried, Z. Phys. 130, 214 (1951).
37. A. K. Head and H. Louat, Austr. J. Phys. 8, 1 (1955).
38. H. Conrad, ref. 18, p. 290.
39. J. Meakin and N. J. Petch, Symp. on Role of Substructure, ASD-TDR 63-324, 243, Orlando Florida (1963).
40. J. C. M. Li, Trans. TMS AIME 227, 247 (1963).

41. P. J. Worthington and E. Smith, Acta Met. 12, 1277 (1964).
42. U. F. Kochs, Met. Trans. 1, 1121 (1970).
43. G. Zankl, Z. Naturforsch, 18a, 795 (1963).
44. R. W. Armstrong, I. Codd, R. M. Douthwalter and H. S. Petch, Phil. Mag. 7, 45 (1962).
45. M. J. Marcinkowski and H. A. Lipsitt, Acta Met. 10, 95 (1962).
46. E. S. Meiran and D. A. Thomas, Trans. AIME 233, 937 (1965).
47. F. C. Lindley and R. E. Smallman, Acta Met. 11 626 (1963).
48. M. A. Adams, A. C. Roberts, and R. E. Smallman, Acta Met. 331 (1960).
49. A. M. Omar and A. R. Entwisle, Materials Science and Engineering 5, 263 (1969/70).
50. A. Gilbert, D. Hull, W. S. Owen and C. N. Reid, J. Less-Common Metals 4, 399 (1962).
51. C. L. Formby and W. S. Owen, Phil. Mag. 13, 41 (1966).
52. J. D. Bailon, A. Loyer, and J. M. Dorlot, Materials Science and Engineering 8, 288 (1971).
53. H. Conrad, Can. J. Phys. 45, 581 (1967).
54. C. W. Burnaham, Carnegie Institution of Washington Yearbook 61 (1961-62).
55. R. Stevenson, Ph.D. Thesis, M.I.T. (1972).
56. J. W. Steeds, Proc. Roy. Soc. A292, 343 (1966).
57. P. B. Hirsch et al., Electron Microscopy of Thin Crystals, Butterworths, London (1965).
58. D. A. Vaugh, O. M. Stewart and C. M. Schwartz, Trans. AIME 221, 937 (1961).
59. W. C. Leslie and R. J. Sober, Trans. ASM 60, 459 (1967).

60. J. P. Hirth and M. Cohen, *Met. Trans.* 1, 1 (1970).
61. J. W. Pugh, *Trans. Amer. Soc. Metals* 47, 984 (1955).
62. G. T. Hahn, *Acta Met.* 10, 27 (1962).
63. W. G. Johnston and J. J. Gilman, *J. Appl. Phys.* 30, 129 (1959).
64. H. Conrad, Ultrafine-Grain Metals, J. J. Burke and Volkes Weiss, editors, Syracuse University Press, p. 213 (1970).
65. R. L. Jones and H. Conrad, *Trans. Met. Soc. AIME* 11, 239 (1969).
66. A. S. Keh and S. Weissmann, Electron Microscopy and the Strength of Crystals, F. Washburn and G. Thomas, editors, Interscience, p. 257 (1961).
67. R. M. Fisher, Ph.D. Thesis, University of Cambridge (1962).

BIOGRAPHICAL NOTE

The author, William David Rosenberg, son of Mr. and Mrs. Charles Rosenberg of Washingtonville, New York, was born on February 15, 1941 in Troy, New York. After completing his high school education in Averill Park, New York, he entered Rensselaer Polytechnic Institute where in 1963 he was awarded the degree of Bachelor in Metallurgical Engineering.

The next two years were spent working as a mill and melt shop metallurgist for the Crucible Steel Company in Syracuse, New York, while attending Syracuse University at night. In 1965, the author entered Syracuse University where he was awarded the degree of Master of Science in Metallurgy in 1966. That same year he married Rachel Bell of Rutland, Vermont.

The author joined I.B.M. in 1966 where he worked on diffusion process development. Prior to entering M.I.T. in 1969, he was manager of the department for diffusion processes as a project engineer.

He has been elected to Sigma Xi and is a member of the American Society for Metals, the American Institute of Mining, Metallurgical and Petroleum Engineers and the New England Microscopy Society.